Bioorganic Chemistry 134 (2023) 106455

Contents lists available at ScienceDirect

Bioorganic Chemistry

journal homepage: www.elsevier.com/locate/bioorg

Evaluation of honokiol, magnolol and of a library of new nitrogenated neolignans as pancreatic lipase inhibitors

Claudia Sciacca, Nunzio Cardullo, Luana Pulvirenti, Antonella Di Francesco, Vera Muccilli *

Department of Chemical Sciences, University of Catania, V.le A. Doria 6. 95125, Catania, Italy

ARTICLE INFO

Keywords:
Antiobesity drugs
Natural products
Pancreatic lipase
Enzyme Inhibition
Honokiol
Magnolol
Suzuki-Miyaura cross coupling
Biphenyls
Lignans and neolignans

ABSTRACT

Obesity is a complex disease defined as an excessive amount of body fat. It is considered a risk factor for several pathologies; therefore, there is an increasing interest in its treatment. Pancreatic lipase (PL) plays a key role in fat digestion, and its inhibition is a preliminary step in the search for anti-obesity agents. For this reason, many natural compounds and their derivatives are studied as new PL inhibitors. This study reports the synthesis of a library of new compounds inspired by two natural neolignans, honokiol (**1**) and magnolol (**2**) and bearing amino or nitro groups linked to a biphenyl core. The synthesis of unsymmetrically substituted biphenyls was achieved through an optimisation of the Suzuki-Miyaura cross-coupling reaction followed by the insertion of allyl chains, thus furnishing the *O*- and/or *N*-allyl derivatives, and finally, a sigmatropic rearrangement yielding in some cases, the *C*-allyl analogues. Magnolol, honokiol and the twenty-one synthesised biphenyls were evaluated for their in vitro inhibitory activity toward PL. Three compounds (**15b**, **16** and **17b**) were more effective inhibitors than the natural neolignans (magnolol IC_{50} = 158.7 μM and honokiol IC_{50} = 115.5 μM) with IC_{50} of 41–44 μM. Detailed studies through kinetics suggested better inhibitory activity of the synthetic analogues compared with the natural **1** and **2**. Magnolol (K_i = 614.3 μM; K'_i of 140.9 μM) and the synthetic biphenyls **15b** (K_i = 286.4 μM; K'_i = 36.6 μM) and **16** (K_i = 176.2 μM; K'_i = 6.4 μM) are mixed-type inhibitors, whereas honokiol (K_i = 674.8 μM) and **17b** (K_i = 249 μM) are competitive inhibitors. Docking studies corroborated these findings, showing the best fitting for intermolecular interaction between biphenyl neolignans and PL. The above outcomes highlighted how the proposed structures could be considered interesting candidates for future studies for the development of more effective PL inhibitors.

1. Introduction

Obesity is a complex condition involving an excessive amount of body fat. This pathology is not only an aesthetic problem but also determines abnormal physiological metabolism. Obesity is a significant risk factor for several diseases, such as hypertension and cardiovascular diseases [1], hyperlipidemia, diabetes [2], and cancer[3]. The European Commission has recently classified obesity as a chronic, relapsing disease [4]. The treatment of obesity relies on long-term dietary regulation, exercise intervention, short-term drug treatment and surgery (liposuction) [5]. Amongst the several targets investigated for treating or preventing obesity, pancreatic lipase (PL) inhibition is considered successful because of its tolerable side effects [6]. PL plays a key role in dietary fat digestion by converting triacylglycerols into 2-monoacylglycerols and free fatty acids in the intestine that the body can absorb and participate in metabolism. The inhibition of this enzyme achieves a lipid-lowering effect, thus controlling fat entering the blood. Orlistat (Xenical) is the only approved anti-obesity drug. However, some side effects, such as flatulence, faecal incontinence, and steatorrhea, have been reported [7,8]. For this reason, synthetic and natural compounds have been studied to find new and safe enzyme inhibitors with no or low side effects. For example, a series of bis(sulfonate) derivatives [9], benzothiazole sulfonate derivatives bearing azomethine [10] and Pd(II)-Schiff base complexes [11] were evaluated as new pancreatic lipase inhibitors.

Natural products from traditional medicinal plants and microbial origin are important sources of novel drug leads. Traditional Chinese medicinal herbs are a rich source of lead compounds and are possible drug candidates to treat a pathological condition such as obesity. Recently, honokiol (**1**, Fig. 1), a bisphenolic neolignan isolated from *Magnolia officinalis* leaves, was studied as responsible for the lipase inhibitor activity of the extract [12]. For this reason, further investigations

* Corresponding author.
E-mail address: v.muccilli@unict.it (V. Muccilli).

https://doi.org/10.1016/j.bioorg.2023.106455
Received 27 December 2022; Received in revised form 16 February 2023; Accepted 1 March 2023
Available online 6 March 2023

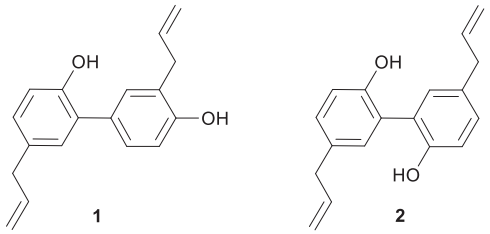

Fig. 1. Natural bioactive neolignans honokiol (**1**) and magnolol (**2**).

are necessary. Moreover, the presence of magnolol (**2**), together with **1** is frequently associated with the pharmacological effects of various remediation obtained by extraction/decoction from *Magnolia* spp.[1]. In particular, **1** and **2** have been studied as having anticancer, antistress, anti-anxiety, antidepressant, antioxidant, anti-inflammatory and hepatoprotective effects [13–15]. The high combination of biological activities makes magnolol and honokiol promising natural scaffolds for discovering new therapeutic agents. Studies on the structure–activity relationship (SAR) have shown that some of the biological properties of **1** and **2** are related to the simultaneous presence of hydroxyl and allyl groups on the biphenyl core [16,17].

Several research papers have been devoted to the synthesis of structural analogues of **1** and **2** and the evaluation of their biological properties: this afforded new bisphenol neolignans with anticancer activity as tankyrase-2 inhibitors [18] and inhibitors of tumour cells growth [19], hypoglycemic activity [20], antibacterial activity toward *Staphylococcus aureus*, *Methicillin-resistant S. aureus* and *Vancomycin-resistant Enterococcus* [21], antiproliferative activity inhibiting in vitro migration and capillary-like tube formation in Human Umbilical Vein Endothelial Cells (HUVECs) [22], and $GABA_A$ receptor modulators with a promising role in neuroprotection [23].

This research describes a detailed investigation of the PL inhibitory activity of honokiol, considered a suitable candidate for the treatment of obesity [12] but lacking a deep in vitro analysis of the inhibition mechanism. This study was consequently extended to magnolol in light of their structural similarity. Indeed, it is known that obesity is connected to other metabolic disorders, including diabetes. For this reason, the evaluation of **1** and **2** as PL inhibitors may be relevant as they have been studied as inhibitors of other metabolic enzymes (i.e. α-glucosidase and α-amylase [20,24]).

In addition, we obtained a library of new biphenyl neolignans inspired by honokiol and magnolol, bearing amino or nitro groups and synthesised by an optimised Suzuki-Miyaura (SM) cross-coupling reaction to investigate similar structure suitable for PL inhibition. The choice of inserting amino and nitro groups is related to previous findings on bioactive compounds bearing those functional groups [25] which were among the most active lipase inhibitors among those studies. A deep insight by in silico study has shown as those functions are involved in stabilising ligand–protein complex by forming hydrogen bonds with aminoacid residues of catalytic site of lipase (Ser-152, His-263 and Phe-77) [25]. Furthermore, in the occurrence of positive results, these represent suitable groups for further derivation.

2. Results and discussion

2.1. Synthetic procedure

Scheme 1 shows the synthetic strategy designed to yield new nitrogenated biphenyls inspired by bioactive magnolol and honokiol. Namely, the Suzuki-Miyaura cross-coupling reaction was employed to afford new biphenyl compounds, followed by nucleophilic substitution and sigmatropic rearrangement to insert allyl chains into the biphenyl core.

For the SM reaction, the reagents reported in Fig. 2 were employed, and the bromide **3a** and pinacol boronic ester **4a** were used as model compounds to optimise the reaction conditions. Selected experiments were conducted to yield the biphenyl **5** employing Pd-based catalysts with different ligands and solvents (see Table 1). Specifically, $Pd(PPh_3)_4$ was employed as a catalyst, whereas the precatalyst $Pd(OAc)_2$ was used in combination with ligands 1,1′-bis(biphenylphosphino)ferrocene (Dppf) or 2-dicyclohexylphosphino-2′,6′-dimethoxybiphenyl (SPhos) to generate in situ the active form. The amount of catalyst and ligand was varied by employing the latter in molar percentage twice the former.

According to the results, conventional SM reaction conditions, namely the use of $Pd(PPh_3)_4$ or $Pd(OAc)_2$/Dppf, gave poor results when employed on this substrate. The expected compound **5** was isolated with a 10% yield only in the conditions reported in entry 3 of Table 1. These results suggest the dialkylbiarylphosphines based catalysts, usually employed with aryl halides and boronic acids, may be inefficient when substituted bromoaniline reacts with boronic acid pinacol esters, as pointed out by Reizman et al. also [26].

Conversely, the employment of SPhos in combination with $Pd(OAc)_2$ was more effective in the synthesis of biphenyl **5**. The expected product was obtained in higher yields (25.2–33.6%; entries 5 and 7) when the reaction was carried out in THF rather than toluene. Moreover, the yield was notably improved (from 33.6 to 98%) when a mixture of THF: H_2O (10:1) was employed (entry 8). According to Altman et al., SPhos generates highly active and stable catalyst systems, thus justifying the encouraging results [27]. Furthermore, the SPhos-based catalyst promotes the reaction of electron-rich aryl halides with excellent yields (>90%), and allows the synthesis of highly hindered diaryls containing large *ortho,ortho'*-substituents [28]. Further experiments were performed to lower the amount of precatalyst and ligand, as pointed out in

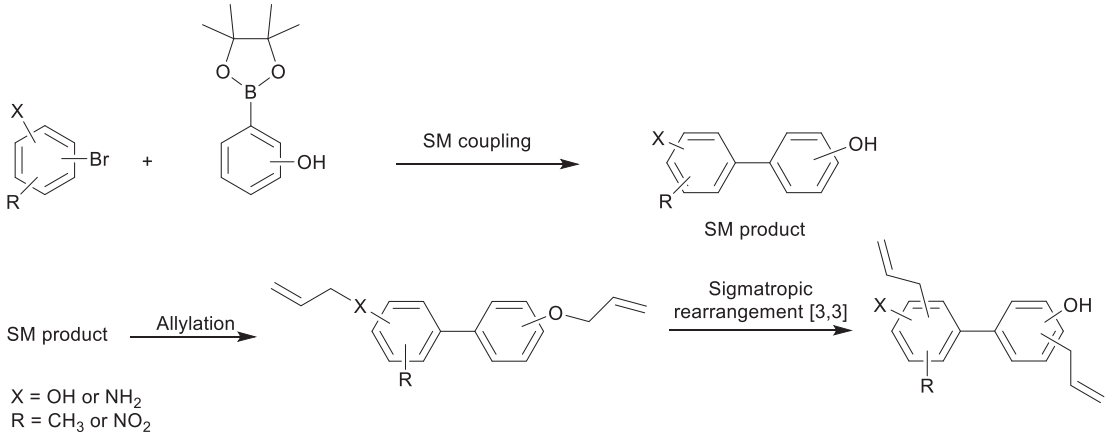

Scheme 1. Synthetic strategy proposed to achieve nitrogenated biphenyls inspired by **1** and **2**.

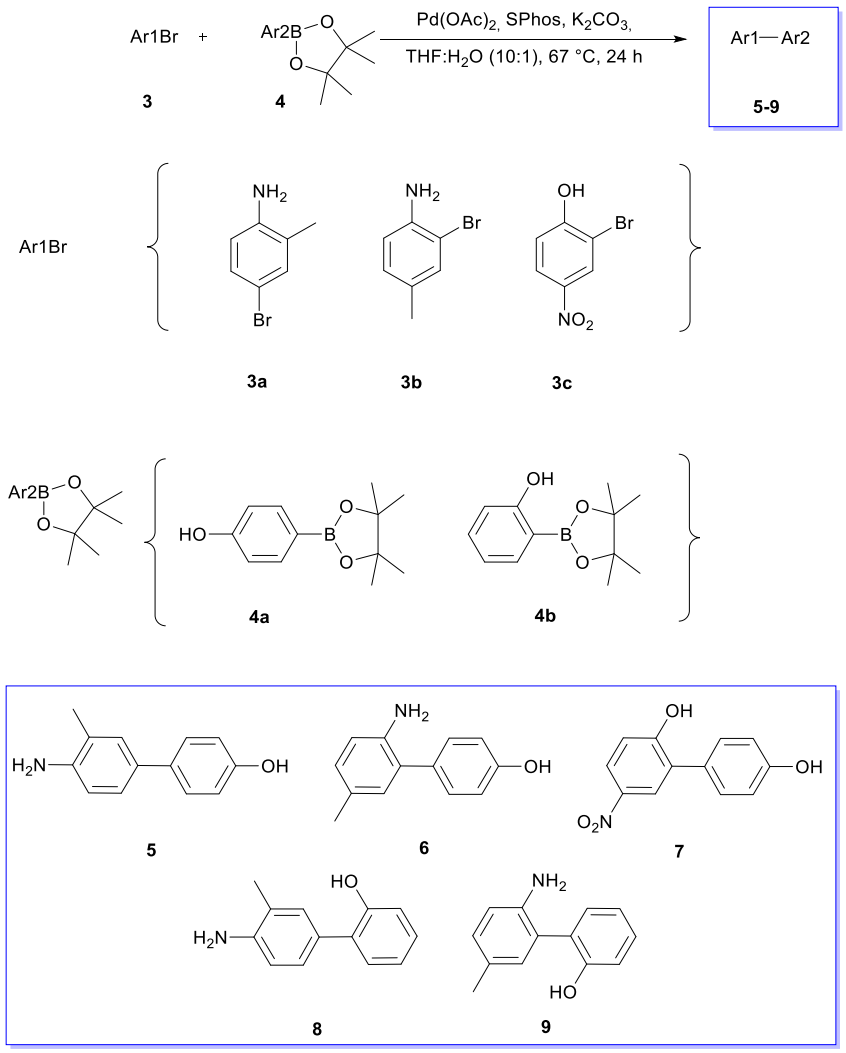

Fig. 2. Synthesis of biphenyls **5**–**9**.

Table 1
Substrate scope of SM cross-coupling of **3a** with **4a**.

Entry	Catalyst	mol%[a]	Ligand	mol%[a]	Solvent	T (°C)	Time	%yield[b]
1	$Pd(PPh_3)_4$	8	–	–	THF	67	24 h	0
2	$Pd(OAc)_2$	5	Dppf	15	THF-H_2O[c]	67	24 h	0
3	$Pd(OAc)_2$	10	Dppf	30	THF-H_2O[c]	67	24 h	10[d]
4	$Pd(OAc)_2$	1	SPhos	2	dry Toluene	80	22 h	8
5	$Pd(OAc)_2$	1	SPhos	2	THF	67	22 h	25.2
6	$Pd(OAc)_2$	10	SPhos	20	dry Toluene	80	22 h	15
7	$Pd(OAc)_2$	10	SPhos	20	THF	67	22 h	33.6
8	$Pd(OAc)_2$	10	SPhos	20	THF-H_2O[c]	67	3 h	98
9	$Pd(OAc)_2$	5	SPhos	10	THF-H_2O[c]	67	5 h	96.4
10	$Pd(OAc)_2$	1	SPhos	2	THF-H_2O[c]	67	24 h	98.7

[a] referred to aryl halide **3a**.
[b] determined by HPLC-UV quantification (see experimental section).
[c] THF-H_2O (10:1).
[d] determined after column chromatography (see experimental section).

entries 9 and 10. According to these findings, the reduction of the catalyst amount employed does not negatively affect the reaction yield, affording the biphenyl **5** in almost quantitatively yield, although with a longer reaction time. Based on these data, we have employed the latter conditions (entry 10) for the synthesis of other biphenyl compounds, preferring long reaction times over catalyst loading. The new biphenyls obtained with a 70 – 97% yield (**5** – **8**) are listed in Fig. 2; the biphenyl **9**, reported by Cho et al.[29] was obtained with a 65% yield.

The compounds **5** – **9** were subjected to two further reaction steps to insert allyl chains onto the biphenyl core. Firstly, allyl bromide furnished the *O*- and/or *N*-allyl derivatives (Scheme 2). A total of ten allylated derivatives were obtained and, subsequently, were subjected to sigmatropic rearrangement. The details of the two reactions and the obtained products are reported in Scheme 2. Claisen rearrangement of

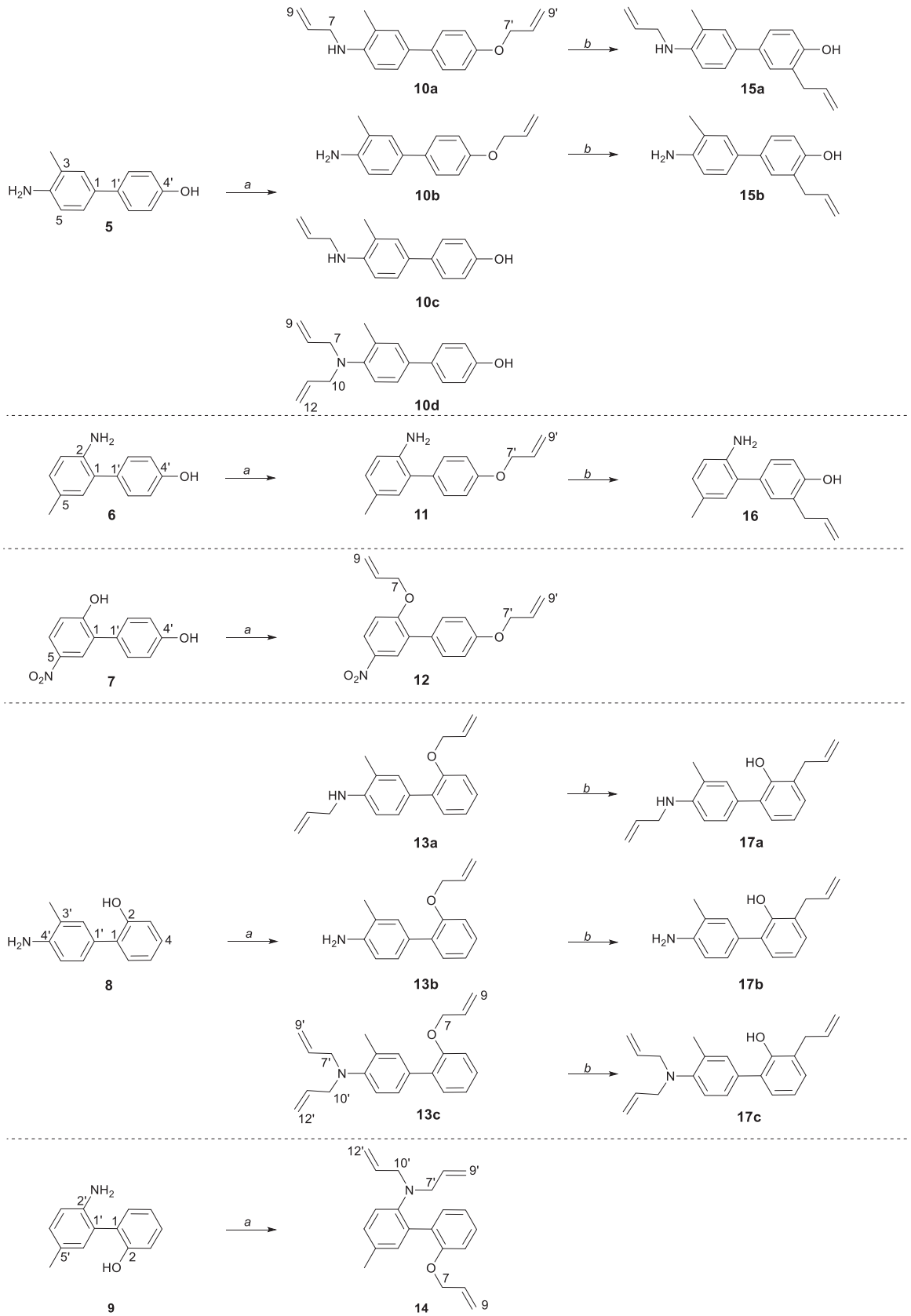

Scheme 2. Synthesis of biphenyls **10**–**17**. *a)* dry acetone, K_2CO_3, allyl bromide, 56 °C. *b*) dry CH_2Cl_2, 1 M $(Et)_2AlCl$ (in dry *n*-hexane), room temperature.

O-allyl chains occurred in mild reaction conditions (room temperature) as the presence of diethyl aluminium chloride promotes the process, avoiding the high temperatures typically used [30]. The Claisen reaction conditions were inefficient for rearranging *O*-allyl chains in **12** and **14** and for all *N*-allyl chains. Moreover, the employment of the reaction conditions generally reported for aza-Cope rearrangement [31–33] of *N*-allylanilines was unsuccessful (see Supplementary Information for details). Furthermore, the strategy to insert *C*-allyl chains via SM reaction before the SM step was discarded as palladium causes isomerisation of double bound, yielding a complex mixture of *cis* and *trans* isomers difficult to purify [34].

2.2. In vitro pancreatic lipase inhibitory activity

The inhibition of the PL enzyme was established employing spectrophotometric methodologies previously described [35,36]. The inhibitory activity was expressed as the concentration inhibiting the 50% of enzyme activity (IC_{50}; μM); thus, the lower the IC_{50} value, the higher the inhibitory activity. The data obtained for PL are reported in Table 2. The anti-obesity agent orlistat, a PL inhibitor, is used as a positive reference in the assays.

According to these results, all the biphenyl compounds obtained by SM cross-coupling (**5** – **9**) are inactive (>300 μM) or weak inhibitors (100–300 μM) of the enzyme. In contrast, the *O* and/ or *N*-allyl derivatives (**10** – **14**) and even more the products of Claisen rearrangement (**15** – **17**) are more effective inhibitors. Generally, among the allylated derivatives, compounds bearing free NH_2 and OH groups are the most active inhibitors. Thus, the potency of inhibition increases from the biphenyl to the corresponding *O*-allyl derivative with free NH_2 and to the *C*-allyl derivative with free NH_2 and OH. Namely, along a series (constituted by the same biphenyl skeleton), the order of inhibitory activity is **5** (225.5 μM) < **10b** (46.9 μM) ≤ **15b** (41.7 μM); **6** (180.0 μM > 300 μM) < **11** 106.1 μM) < **16** (42.6 μM); **8** (>300 μM,) < **13b** (82.6 μM) < **17b** (44.4 μM).

An overall sight of the results pinpoints the bisphenols **15b, 16** and **17b** as promising PL inhibitors (<45 μM). A structural trait of these compounds, in addition to free OH groups, is the presence of an allyl chain in the *ortho* position to a phenolic group, a typical structural feature of honokiol. Moreover, the IC_{50} values of these compounds are lower than those observed for **1** and **2** (115.5 μM and 158.7 μM, respectively). Thus, **15b**, **16**, and **17b** are more effective inhibitors than the natural **1** and **2**. It is clear that the IC_{50} values of **15b, 16** and **17b** are poor compared to Orlistat (Table 2); however, their structural features are worthy of note for the development of new anti-obesity drugs.

Table 2
Inhibitory activity (IC_{50}) of PL.

ID	IC_{50} (μM) ± SD
1	115.5 ± 9.0^{c}
2	158.7 ± 5.1 ^{h}
5	225.5 ± 11.0^{a}
6	180.0 ± 13.0^{b}
7	113.2 ± 1.7^{c}
8	>300
9	103.6 ± 19^{c,d,e}
10a	53.7 ± 0.2^{f,g}
10b	46.9 ± 1.4 ^{g}
10c	76.6 ± 7.0^{e,f}
10d	45.6 ± 5.0 ^{g}
11	106.1 ± 7.8^{c,d}
12	47.8 ± 2.1 ^{g}
13a	119.0 ± 6.9^{c}
13b	82.6 ± 2.9^{d,e}
13c	93.2 ± 9.4^{c,d,e}
14	57.0 ± 2.3 ^{g}
15a	54.0 ± 1.3^{f,g}
15b	41.7 ± 1.5 ^{g}
16	42.6 ± 2.0^{f,g}
17a	53.5 ± 6.4^{f,g}
17b	44.4 ± 1.4 ^{g}
17c	93.2 ± 13.5^{c,d,e}
Orlistat	0.9 ± 0.1 ^{h}

The IC_{50} values are mean ± SD (n = 3). Values with the same letters are not significantly different at $P <$ 0.01 (Tukey test).

Thus, the biphenyls **15b, 16** and **17b** were subjected to an in silico ADME study on the SwissADME web platform [37]. The analysis (Figures S128 – S130) highlighted good physicochemical properties such as lipophilicity and topological polar surface area [38]. Although these biphenyls show poor/low water solubility, a good bioavailability score [39] and a favourable drug-likeness profile without violation of the most common rule-based filters (Lipinski, Veber, Ghose) were calculated [37]. The molecules have low skin permeation, but the prediction indicates high gastrointestinal absorption. Finally, none of these molecules has been identified as PAINS (pan assays interference compounds) [37]. Furthermore, functional groups such as $–NH_2$ or NO_2 could be useful for further modifications to improve the ADME properties if they are not relevant to the inhibitory activity of PL.

Biphenyls **15b, 16** and **17b** were selected for a deeper investigation of their PL inhibitory activity together with the natural biphenyl **1** and **2**.

2.3. Kinetics of pancreatic lipase inhibition

The inhibition of PL of the most promising inhibitors **15b, 16** and **17b** and of the natural neolignans **1** and **2** were also evaluated through an enzyme kinetics study employing a spectroscopic assay [36]. As detailed in the Experimental Section, the mode of inhibition of **1**, **2**, **15b**, **16** and **17b** on PL was determined through the Lineweaver-Burk (L-B) graphs by plotting the reciprocal of initial velocity (v_0) versus the reciprocal of the substrate (S) concentration (Fig. 3). The kinetic results are listed in Table 3.

However, although natural products **1** and **2** have a very similar structure, according to these findings, they act as PL inhibitors in two different manners. Precisely, **1** is a competitive inhibitor (Fig. 3A) as the L-B plot results in data lines crossed on the y-axis (namely, the inhibitor does not affect the ν_{max} of the reaction). In this case, a K_i value of 674.8 μM for the enzyme-inhibitor complex (EI) formation was determined by plotting the slope of L-B plot lines vs the inhibitor concentration (Figure S131). Differently, **2** is a mixed-type inhibitor (Fig. 3B) with data lines on the L-B plot intersected in the third quadrant. This behaviour can be explained by an intermediate mechanism between non-competitive and uncompetitive inhibition, the latter being prevalent [35]. In this particular case, the K'_i should be less than K_i, where K'_i and K_i are the inhibitor constants for the formation of ESI complex and EI complex, respectively. The secondary plots of the L-B plot (Figure S131) confirmed the above-described processes with K_i of 614.3 μM and K'_i of 176.2 μM.

The kinetic data of the synthetic biphenyls **15b** and **16** suggested a mixed-type inhibition (Fig. 3C and 3D) as found for **2**. Namely, also these two compounds display a mechanism between non-competitive and uncompetitive, with $K'_i < K_i$ as confirmed by secondary plots. Worthy of note, the two biphenyls gave lower dissociation constants with respect to those observed for magnolol (**2**). In particular, **16** is a promising inhibitor with a high affinity for the ES complex, as suggested by the low micromolar K'_i value of 6.4 μM.

The analysis of the Lineweaver-Burk plots for PL inhibition in the presence of **17b** (Fig. 3E) indicated a competitive inhibition as increasing amounts of inhibitor does not change ν_{max} (0.31 ± 0.03 ΔOD/min). A K_i of 249.0 μM was determined by plotting the slope of each line of L-B plot vs the concentration of the inhibitor.

2.4. Molecular docking study

A molecular docking study investigated the affinity for the pancreatic lipase catalytic site of the natural honokiol and magnolol and the

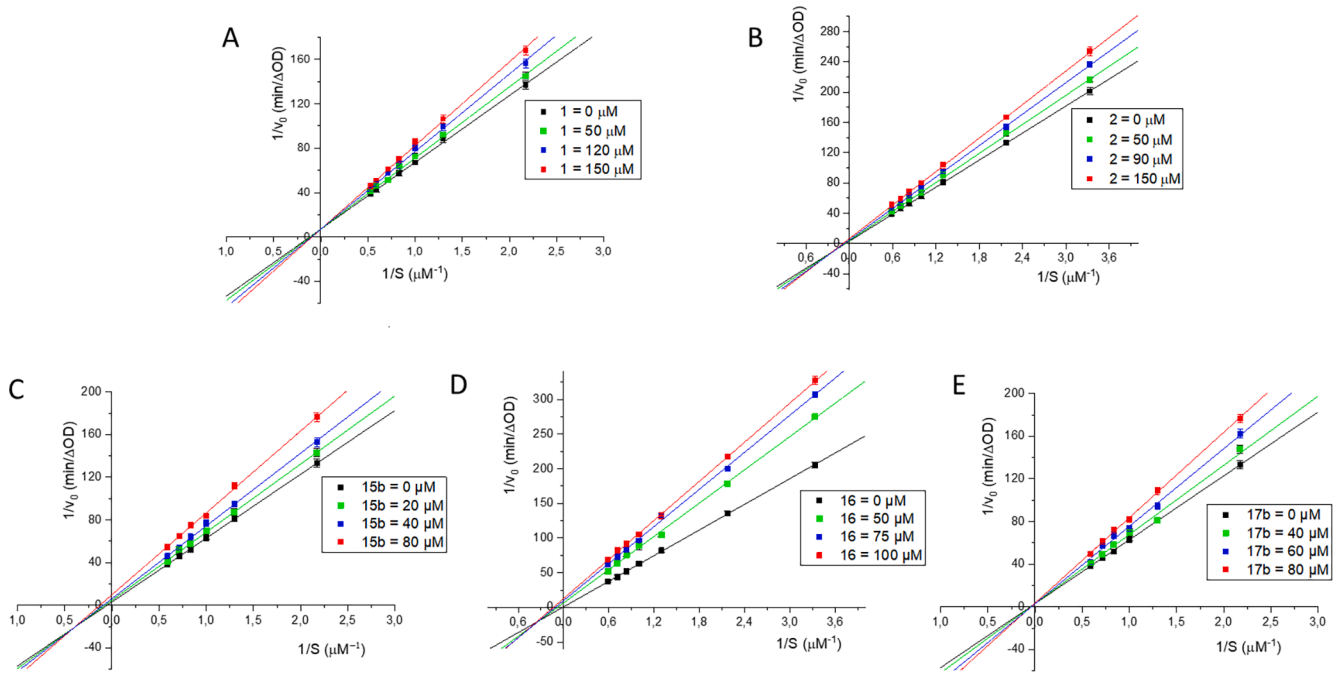

Fig. 3. Lineweaver-Burk plots of **1** (A), **2** (B) and biphenyls **15b** (C), **16** (D) and **17b** (E) with PL.

Table 3
Kinetic parameters for PL inhibition with **1, 2**, **15b**, **16** and **17b**.[a.]

compound	PL		
	Type of inhibition	K_i = ± S.E.M. (μM)	K'_i= ± S.E.M. (μM)
1	competitive	674.8 ± 43.1	–
2	mixed-type	614.3 ± 19.1	140.9 ± 8.6
15b	mixed-type	286.4 ± 20.5	36.6 ± 2.3
16	mixed-type	176.2 ± 13.8	6.4 ± 1.4
17b	competitive	249.0 ± 34.6	–

[a] K_i refers to the constants for the formation of EI complex; K'_i refers to the constant for the formation of ESI complex.

biphenyls **5 – 17**, thus suggesting a better understanding of the inhibition mechanism.

The key interacting residues in the binding site of PL include Ser152, Phe215, Arg256, His263, Leu264, Asp176 and Tyr114 [36]. The computational experiments were acquired employing Autodock Vina and Glide Ligand Docking (See the Experimental Section for more details).

The visualisation of docking outcomes showed that ligands are well accommodated into the binding pocket, occupying almost the same spatial portion.

A good affinity of this class of nitrogenated inhibitors was suggested

Table 4
Binding Energies (ΔG_{bind}) and Interacting Residues of honokiol (**1**), magnolol (**2**) and bisphenols **5** – **17c** with PL Catalytic Site.[a.]

Ligands	**autodock Vina calcd ΔG_{bind}**	**Glide calcd ΔG_{bind}**	**Interacting residues**
1	−8.6	−6.62	Phe77, Phe215
2	−8.7	−5.55	His263
5	−7.4	−5.15	Gly76, His151, Asp79, His263
6	−7.7	−5.23	His151, Gly76, Asp79, His263, Phe215
7	−7.6	−5.18	Gly76, His151, Asp79
8	−8.1	−6.16	Ser152, Phe77, Asp79
9	−8.2	−5.38	His263
10a	−7.6	−3.39	His263, Ser152
10b	−7.7	−5.19	His263
10c	−7.8	−4.95	His263
10d	−7.3	−3.98	His263
11	−8.1	−5.48	His263
12	−7.6	−4.47	Arg256, His151
13a	−7.1	−3.89	His263
13b	−7.3	−4.92	His263
13c	−7.0	−5.30	Phe77
14	−6.5	−4.45	–
15a	−8.4	−3.88	His263
15b	−8.4	−5.51	Phe77, His263, Asp79
16	−8.5	−5.70	Phe77, His263
17a	−7.8	−4.77	Phe77, His263
17b	−8.0	−6.71	Phe77, Phe215, His263
17c	−7.7	−6.58	Phe77, Ser152
Orlistat	−6.6	−3.45	His263

[a] The ΔG_{bind} values were calculated with Autodock Vina and Glide and are expressed as Kcal/mol.

Table 5
List of molecular interactions of **1**, **2**, **5** – **17c** with PL Catalytic Site.[a.]

Ligands	Interacting residues	Interaction	Distance (Å)
1			
B-ring	Phe77	π – π	–
O2′(B-ring)	Phe77	H-donor	2.0
B-ring	Phe215	π – π	–
2			
A-ring	His263	π – π /π - cation	–
5			
O4′ (B-ring)	Gly76	H-acceptor	2.6
O4′ (B-ring)	His151	H-acceptor	2.1
O4′ (B-ring)	Asp79	H-donor	1.8
B-ring	His263	π - π	–
6			
O4′ (B-ring)	Gly76	H-acceptor	2.7
O4′ (B-ring)	His151	H-acceptor	2.1
O4′ (B-ring)	Asp79	H-donor	1.8
B-ring	His263	π – π/ π - cation	–
A-ring	Phe215	π - π	–
7			
O4′ (B-ring)	Gly76	H-acceptor	2.6
O4′ (B-ring)	His151	H-acceptor	2.1
O4′ (B-ring)	Asp79	H-donor	1.8
8			
O2 (B-ring)	Ser152	H-donor	1.8
B-ring	Phe77	π - π	–
N4′ (A-ring)	Asp79	H-donor	2.8
9			
B-ring	His263	π - π	–
B-ring	His263	π - cation	–
10a			
A-ring	His263	π - π	–
N4 (A-ring)	Ser152	H-donor	2.2
10b			
B-ring	His263	π – π/ π - cation	–
10c			
A-ring	His263	π – π/ π - cation	–
10d			
B-ring	His263	π – π	–
11			
B-Ring	His263	π – π/ π - cation	–
12			
O4′ (B-ring)	Arg256	π - cation	–
A-ring	His151	salt bridge	–
13a			
A-ring	His263	π – π/ π - cation	–
13b			
A-ring	His263	π – π/ π - cation	–
13c			
B-ring	Phe77	π – π	–
14			
–	–	–	–
15a			
A-ring	His263	π – π/ π - cation	–
15b			
A-ring	Phe77	π – π	–
B-ring	His263	π – π/ π - cation	–
O4′(B-ring)	Asp79	H-donor	2.0
16			
A-ring	Phe77	π – π	
B-ring	His263	π – π/ π - cation	
O4′ (B-ring)	Asp79	H-donor	2.4
17a			
O2′(B-ring)	Phe77	H-donor	2.3
B-ring	His263	π - cation	–
17b			
O2 (B-ring)	Phe77	H-donor	1.8
A/B-ring	Phe215	π – π	–
A-ring	His263	π – π	–
N4′ (A-ring)	Tyr114	H-donor	2.5
17c			
B-ring	Phe77	π – π	–
O2(B-ring)	Ser152	H-donor	2.1
orlistat			
	His263	H-acceptor	2.6

[a] Otherwise indicated in Fig. 4, the A-ring brings amino or nitro group, B-ring is the phenolic ring.

by the calculated binding energies (Kcal/mol) listed in Table 4. The visual inspection of docked conformation allowed us to determine a list of molecular interactions for each analysed compound reported in Table 5.

The analysis of docked poses allowed us to highlight the main interacting residues that can stabilise the complex of the compounds under evaluation with PL; non-covalent interactions are mainly established with His263, His151, Ser152, Asp79, Gly76, Phe215, Arg256 and Phe77 that surround the skeleton of the ligands into the catalytic pocket. This study suggests that His263 could play a key role in the interactions with this class of inhibitors, together with Phe77 and Phe215. Some considerations about the skeleton of the biphenyl neolignans as important structural features to stabilise the complex with PL can be inferred. For instance, the B-ring bearing the free hydroxyl group in C-2′ or C-4′ position is involved in interactions with the residues in the binding cavity. In contrast, the A-ring, bringing an amino or nitro group, was less involved and allowed to establish only weak contact with the protein counterpart when bearing more bulky substituents, probably due to the conformation geometry of the ligand into the cavity.

Among the compounds under evaluation, **15b**, **16,** and **17b** showed the best fitting for intermolecular interactions with PL. By the 2D interaction diagrams reported in Fig. 4, it was possible to visualise that the compounds **15b**, **16** and **17b** are accommodated into the binding pocket in a way the A-ring (containing the amino group) is surrounded by the hydrophobic residues Leu264, Tyr267, Pro180, Ala178, Ile209, Tyr114, Phe77 and Ile78. Conversely, the B-ring (the phenolic ring) of **17b** is in a positively charged portion, whereas that of **15b** and **16** is in a negatively charged area. The visual inspection of the pose of **15b** and **16** into the cavity (Fig. 4, Figure S123) shows that the B-ring is involved in a π-π stacking and π-cation interactions with His263 while the A-ring forms a π-π stacking interaction with Phe77. In addition to the stabilising interaction, compound **15b** establishes a hydrogen bond with Asp79 through the OH (Fig. 4, Figure S123). Magnolol shares with **15b** and **16** the interaction with His263. The pose of **17b** shows the A-ring interacting with Phe215 and His263 respectively with two π-π stacking interactions, the B-ring interacting also with Phe215 by π-π stacking interaction and the OH involved in a hydrogen bond with Phe77 (Fig. 4, Figure S123). The residue Phe77 is also involved in the stabilisation of the complex PL with **1** through a hydrogen bond with the OH in C-4 and a π-π stacking interaction with the other ring.

The docking analyses grouped the compounds **15b** and **16** with magnolol and **17b** with honokiol, in agreement with kinetic results.

The comparison between **15a** and **15b** allows observing that the derivatisation of NH with an allylic chain at the A-ring changes the orientation into the cavity, and it gets worse the interaction with PL. Also, a comparison between **17a** and **17c,** mono and bis *N*-allyl analogues, respectively, with **17b**, clearly shows a worsening in terms of interactions with PL. In particular, the interaction involving the A-ring is entirely lost; nevertheless, the interaction pattern for the B-ring of both ligands remains good.

Concerning the biphenyl derivatives **5** – **9**, despite the promising interactions calculated and collected in Table 5, the scarce in vitro results towards PL can be explained by the fact that these ligands lack the right lipophilicity. The B-ring of **5** – **9**, lacking the allyl chain of the natural analogues **1** and **2**, remains completely exposed towards the solvent, not generating stabilising interactions. On the other hand, functionalising OH and NH_2 with allyl groups is not a good strategy to improve the affinity with the enzyme, as evidenced by the docking outcomes obtained for the allyl analogues **10a-d**, **11**, **12, 13a-c** and **14.** The results suggest the importance of free OH in the B-ring, in particular when this is in the C-2′ position as for one of the most promising compounds, **17b**; moreover, the allyl chain in *ortho* to the OH would seem important, as mimics the natural distribution of the substituents of the natural compound **1**.

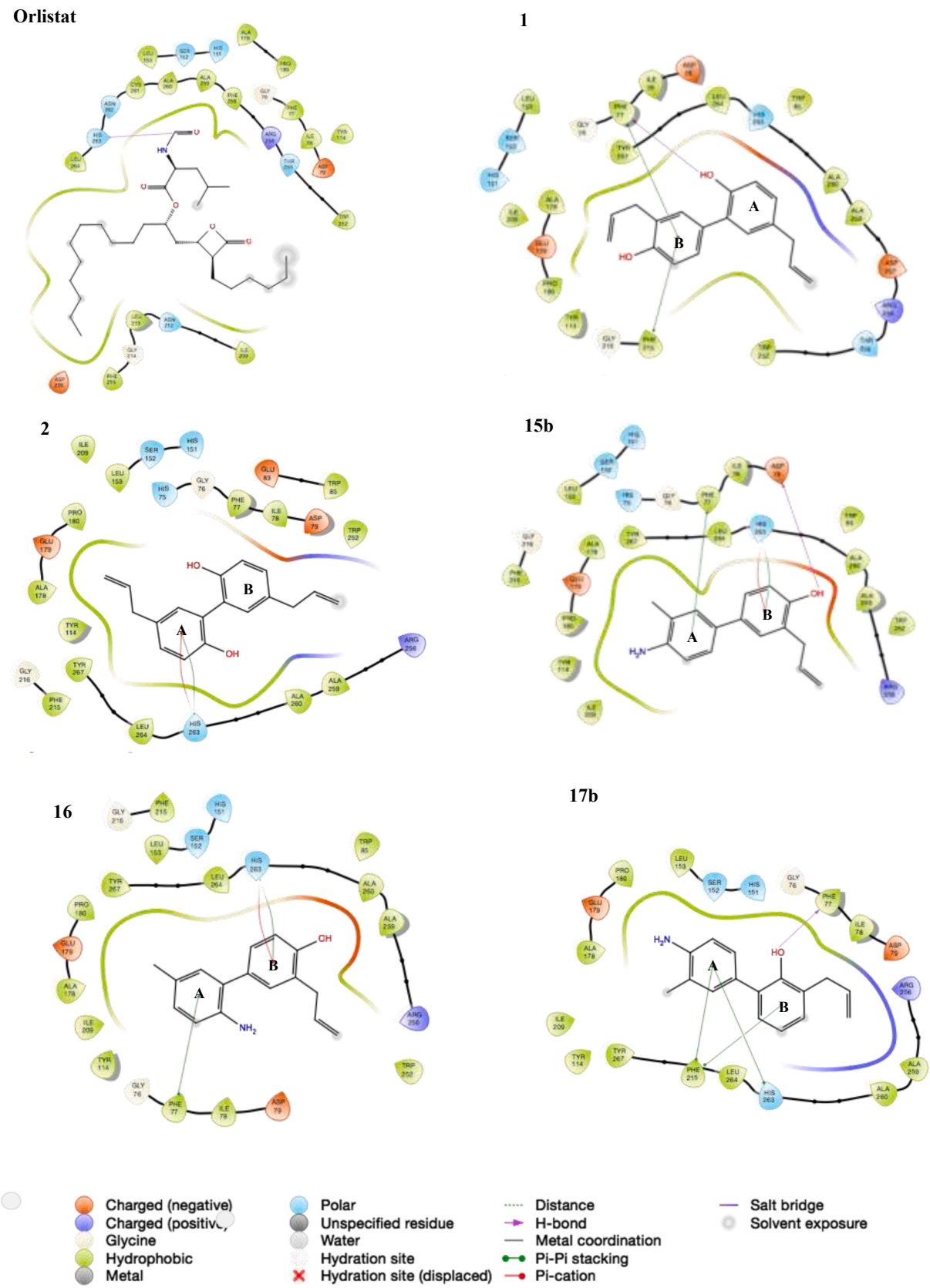

Fig. 4. 2D interaction diagrams of **orlistat**, **1**, **2**, **15b**, **16** and **17b** with PL.

3. Conclusions

In summary, we exploited a synthetic strategy based on the optimisation of Suzuki-Miyaura cross-coupling reaction, followed by two steps based on allylation and a subsequent sigmatropic rearrangement to obtain new biphenyl compounds, including bioinspired neolignans (**15** – **17**). For the first time, a detailed evaluation of pancreatic lipase inhibitory activity was reported here for the natural compounds, honokiol and magnolol, and for new synthetic compounds. Our investigation on the inhibition of the new nitrogenated neolignans showed that three over the twenty-one biphenyls (**15b**, **16** and **17b**) have promising structural features for the development of anti-obesity drugs. The in silico study highlighted the functional groups essential for a good interaction with the enzyme pocket and which functions are detrimental. The significance of this work lies in the high-yield synthetic strategy employed to achieve biphenyls. Since optimising SM cross-coupling conditions to find high-yielding biphenyl structures inspired by natural products is one of the key topics for organic synthetic chemistry, we expect this approach to be of reference value for addressing this challenge. Moreover, up to date, few structures containing nitrogen atoms have been reported with a biphenyl core, despite the biological properties shown by them.

4. Experimental

4.1. General experimental methods

All chemicals were of reagent grade and were used without further purification; tetrahydrofuran (THF) was freshly distilled before being used. NMR spectra were run on a Varian Unity Inova spectrometer operating at 500 MHz (^{1}H) and 125 MHz (^{13}C). Chemical shifts (δ) are indirectly referred to TMS using residual solvent signals (*δ* 3.31 for CD_3OD, 7.26 for $CDCl_3$). Coupling constants (*J*) are reported in Hertz (Hz), and multiplicity in ^{1}H NMR spectra are abbreviated as follows: s for singlet, d for doublet, t for triplet, q for quartet, p for pentet, dd for double doublet, bs for broad singlet, ddd for double double doublet, m for multiplet. All NMR experiments, including two-dimensional spectra, i.e., g-COSY, g-HSQCAD, and g-HMBCAD, were performed using software supplied by the manufacturer and acquired at constant temperature (300 K). g-HMBCAD experiments were optimised for a long-range ^{13}C–^{1}H coupling constant of 8.0 Hz. High-resolution mass spectra were acquired with a Q Exactive Orbitrap mass spectrometer (Thermo Fisher Scientific, Bremen, Germany) equipped with an E.S.I. ion source operating in positive or in negative mode. Samples were dissolved at 1E-5 M concentration in 50:50 (MeOH/H_2O + 1% formic acid) and directly infused in the mass spectrometer. High-performance liquid chromatography (HPLC) was carried out using an Agilent 1100 Series with an autosampler, pump and a diode array UV detector. Preparative liquid chromatography (LC) was performed on silica gel (63–200 μm, Merck, Darmstadt, Germany), Sephadex-LH20 (Sigma-Aldrich, Milan, Italy), or RP-18 (Merck, Darmstadt, Germany) using different mixtures of solvents, as reported below for each compound. Thin layer Chromatography (TLC) was carried out using pre-coated silica gel F254 plates (Macherey-Nagel). The visualisation of reaction components was obtained under UV light at wavelengths of 254 nm and by staining with a solution of cerium sulfate followed by heating. The lipase (PL) inhibition assays were performed on a 96-well microplate, and the Synergy H1 microplate reader was used. Selected compounds (**1**, **2**, **15b**, **16**, **17b**) were analysed by HPLC-UV performed on Chiralcel OD column (4.6 mm × 250 mm, 5 μm, Daicel, Japan), eluted in isocratic mode (*n*-hexane: propan-2-ol 80:20) at 0.7 mL/min, at 10 °C and 27 °C. The chromatograms (acquired at 254 nm) are reported as Supplementary material (Figures S133 and S134).

4.2. Synthesis

4.2.1. Preliminary reaction for the synthesis of 4-amino-3-methyl- [1,1′-biphenyl] −4′-ol (5)

Preliminary experiments for SM reaction were performed employing 4-bromo-2-methylaniline (**3a**; 10.0 mg; 54 μmol) in the presence of 4-(4,4,5,5-tetramethyl-1,3,2-dioxaborolan-2-yl)phenol (**4a;** 11.2 mg; 81 μmol). The solvent, temperature, ligand, and catalyst were varied, as reported in Table 6**.** The reaction yield (reported in Table 6) was determined after quantification with HPLC-UV using a reversed-phase column (RP-18) with the following gradient of CH_3CN/H^+ (99:1 v/v; B) in H_2O/H^+ (99:1 v/v; A) at 1 mL/min: t_0 min B = 10%, t_{20} min B = 100%. The diode array detector was set at 254, 280, and 305 nm. The quantification occurred at 280 nm.

4.2.2. Optimised procedure for preparation of biphenyl neolignans 5 – 9

4-Amino-3-methyl-(1,1′-biphenyl)-4′-ol (5). According to the general procedure, the reaction of **3a** (100.0 mg; 0.54 mmol) with **4a** (178.2 mg; 0.81 mmol) afforded compound **5** (85.0 mg, 79 % yield), after purification on a silica gel column chromatography (dichloromethane → dichloromethane: methanol 98:2). White amorphous solid. ^{1}H NMR (500 MHz, CD_3OD-$CDCl_3$): *δ* 7.38 (d, *J* = 7.9 Hz, 2H, H-2′/H-6′), 7.24 (s, 1H, H-2), 7.22 (d, *J* = 8.2 Hz, 1H, H-6), 6.86 (d, *J* = 7.3 Hz, 2H, H-3′/H5′), 6.75 (d, *J* = 8.1 Hz, 1H, H-5), 2.23 (s, 3H, CH_3). ^{13}C NMR (125 MHz, CD_3OD-$CDCl_3$): *δ* 155.6 (C, C-4′), 143.1 (C, C-4), 133.1 (C, C-1′), 132.1 (C, C-1), 128.7 (CH, C-2), 127.5 (CH, C-2′/C-6′), 125.1 (CH, C-6), 123.1 (C, C-3), 115.7 (CH, C-3′/C-5′), 115.5 (CH, C-5), 17.4 (CH_3). HRESIMS *m/z* 200.1091 $[M + H]^+$, calcd for $C_{13}H_{14}NO$ *m/z* 200.1075.

2-Amino-5-methyl-(1,1′-biphenyl)-4′-ol (6). The reaction of 2-bromo-4-methylaniline (**3b**; 75.0 mg; 0.40 mmol) with **4a** (82.7 mg; 0.60 mmol), afforded compound **6** (60.0 mg, 76 % yield), after purification on silica gel column chromatography (*n*-hexane: acetone 90:10 → 87:13). White amorphous solid ^{1}H NMR. (500 MHz, $CDCl_3$): *δ* 7.27 (d, *J* = 8.0 Hz, 2H, H-2′/ H-6′), 6.96 (d, *J* = 8.1 Hz, 1H, H-4), 6.93 (s, 1H, H-6), 6.88 (d, *J* = 7.9 Hz, 2H, H-3′/H-5′), 6.74 (d, *J* = 8.0 Hz, H-3), 2.20 (s, 3H, CH_3). ^{13}C NMR (125 MHz, $CDCl_3$): *δ* 155.1 (C, C-4′), 139.8 (C, C-2), 131.4 (C, C-1′), 131.1 (CH, C-6), 130.3 (CH, C-2′/C-6′), 128.9 (C, C-5), 128.7 (CH, C-4), 128.3 (C, C-1), 116.4 (CH, C-3), 115.8 (CH, C-3′/C-5′),

Table 6
Preliminary experiments of Suzuki-Miyaura cross-coupling reaction of **3a** with **4a.**

entry	Catalyst	mg, %mol	Ligand	mg, %mol	Solvent (μL)	Base (mmol)	T (°C)	Time(h)
1	$Pd(PPh_3)_4$	4.6, 8%	–		THF (800)	NaOH (0.11)	67	24
2	$Pd(OAc)_2$	0.6, 5%	dppf	4.5, 15%	THF:H_2O (800:80)	K_2CO_3 (0.27)	67	24
3	$Pd(OAc)_2$	1.2, 10%	dppf	9.0, 30%	THF:H_2O (800:80)	K_2CO_3 (0.27)	67	24
4	$Pd(OAc)_2$	0.12, 1%	SPhos	0.5, 2%	dry toluene (100)	K_2CO_3 (0.11)	80	22
5	$Pd(OAc)_2$	0.12, 1%	SPhos	0.5, 2%	THF (100)	K_2CO_3 (0.11)	67	22
6	$Pd(OAc)_2$	1.3, 10%	SPhos	4.9, 20%	dry toluene (100)	K_2CO_3 (0.11)	80	22
7	$Pd(OAc)_2$	1.3, 10%	SPhos	4.9, 20%	THF (100)	K_2CO_3 (0.11)	67	22
8	$Pd(OAc)_2$	1.3, 10%	SPhos	4.9, 20%	THF:H_2O (100:10)	K_2CO_3 (0.11)	67	3
9	$Pd(OAc)_2$	0.12, 1%	SPhos	0.5, 2%	THF:H_2O (100:10)	K_2CO_3 (0.11)	67	24
10	$Pd(OAc)_2$	0.6, 5%	SPhos	2.3, 10%	THF:H_2O (100:10)	K_2CO_3 (0.11)	67	5

20.4 (CH_3). HRESIMS *m/z* 200.1088 $[M + H]^+$, calcd for $C_{13}H_{14}NO$ *m/z* 200.1075.

5-Nitro-(1,1′-biphenyl)-2,4′-diol (7). According to the general procedure, the reaction of 2-bromo-4-nitrophenol (**3c**; 186.0 mg; 0.85 mmol) with **4a** (263.8 mg; 1.30 mmol), afforded compound **7** (138.6 mg, 70 % yield), after purification on a silica gel column chromatography (*n*-hexane: acetone 90:10 → 88:12). Yellow amorphous solid. ^{1}H NMR (500 MHz, CD_3OD-$CDCl_3$): δ 8.13 (d, J = 2.8 Hz, 1H, H-6), 8.00 (dd, J = 8.9 Hz,2.8 Hz, 1H, H-4), 7.41 (d, J = 8.5 Hz, 2H, H-2′/H-6′), 6.92 (d, J = 8.5 Hz, 1H, H-3), 6.86 (d, J = 8.5 Hz, 2H, H-3′/H-5′). ^{13}C NMR (125 MHz, CD_3OD-$CDCl_3$): δ 160.9 (C, C-2), 157.0 (C, C-4′), 140.8 (C, C-5), 130.7 (CH, C-2′/C-6′), 129.5 (C, C-1′), 128.0 (C, C-1), 126.6 (CH, C-6), 124.3 (CH, C-4), 116.1 (CH, C-3), 115.5 (CH, C-3′/C-5′). HRESIMS *m/z* 230.0482 $[M-H]^-$, calcd for $C_{12}H_8NO_4$ *m/z* 230.0453.

4′-Amino-3′-methyl-(1,1′-biphenyl)-2-ol (8). According to the general procedure, the reaction of **3a** (150.0 mg; 0.80 mmol) with **4b** (263.8 mg; 1.20 mmol) afforded compound **8** (160.0 mg, 97 % yield), after purification on a silica gel column chromatography (dichloromethane → dichloromethane: methanol 90:10). White amorphous solid. ^{1}H NMR (500 MHz, $CDCl_3$): δ 7.22 (s,1H, H-2′), 7.19 (d, J = 7.9 Hz, 1H, H-6′),7.17 (d, J = 7.2 Hz, 1H, H-6), 7.06 (t, J = 7.7 Hz, 1H, H-4), 6.84 (t, J = 7.2 Hz, 1H, H-5), 6.84 (t, J = 7.2 Hz, 1H, H-3) 6.75 (d, J = 8.1 Hz, 1H, H-5′), 2.19 (s, 3H, CH_3). ^{13}C NMR (125 MHz, $CDCl_3$): δ 154.9 (C, C-2), 145.0 (C, C-4′), 132.1 (CH, C-2′), 131.3 (CH, C-6′), 130.2 (C, C-1), 130.2 (C, C-1), 128.7 (C, C-6), 128.4 (C, C-4), 123.5 (C, C-3′), 120.6 (CH, C-5), 116.7 (CH, C-3), 116.2 (CH, C-5′), 17.6 (CH_3). HRESIMS *m/z* 200.1089 $[M + H]^+$, calcd for $C_{13}H_{14}NO$ *m/z* 200.1075.

2′-Amino-5′-methyl-(1,1′-biphenyl)-2-ol (9). According to the general procedure, the reaction of **3b** (186.0 mg; 1 mmol) with **4b** (330.0 mg; 1.50 mmol) afforded compound **9** (139.3 mg, 70 % yield) after purification on a silica gel column chromatography (*n*-hexane → *n*-hexane:a cetone 80:20). White amorphous solid. Spectroscopic data were in agreement with those previously reported. [29] HRESIMS *m/z* 200.1075 $[M + H]^+$, calcd for $C_{13}H_{14}NO$ *m/z* 200.1075.

4.2.3. Synthesis of O- and N-allyl derivatives

***N*-Allyl-4′-(allyloxy)-3-methyl-(1,1′-biphenyl)-4-amine (10a) and 4′-(allyloxy)-3-methyl-(1,1′-biphenyl)-4-amine (10b).** A solution of compound **5** (25.0 mg; 0.12 mmol) in dry acetone (2 mL) was mixed in K_2CO_3 (33.2 mg; 0.24 mmol) for 10 min, then, allyl bromide (29.0 mg; 0.24 mmol) was added, and the mixture was refluxed for 6 h. The mixture was filtered, and the expected compound **10a** (17.0 mg, 50 % yield) was recovered after purification on silica gel column chromatography (cyclohexane → cyclohexane: acetone 99:1). Yellow oil. ^{1}H NMR (500 MHz, $CDCl_3$): δ 7.47 (d, J = 8.8 Hz, 2H, H-2′/H-6′), 7.33 (d, J = 8.3 Hz, 1H, H-6), 7.30 (s, 1H, H-2), 6.97 (d, J = 8.8 Hz, 2H, H-3′/H-5′), 6.68 (d, J = 8.3 Hz, 1H, H-5), 6.09 (m, 2H, H-8/H-8′), 5.45 (dd, J = 17.3, 1.5 Hz, 1H, H_a-9′), 5.34 (dd, J = 14.8, 1.4 Hz, 1H, H_a-9), 5.32 (dd, J = 8.4, 1.5 Hz, 1H, H_b-9′), 5.20 (dd, J = 10.4,1.4 Hz, 1H, H_b-9), 4.57 (d, J = 5.4 Hz, 2H, H-7′), 3.88 (d, J = 5.4 Hz, 2H, H-7), 2.24 (s, 3H, CH_3). ^{13}C NMR (125 MHz, $CDCl_3$): δ 157.3 (C, C-4′), 145.0 (C, C-4), 135.5 (CH, C-8), 134.3 (C, C-1′), 133.5 (CH, C-8′), 129.8 (CH, C-1), 128.5 (CH, C-2), 127.3 (CH, C-2′/C-6′), 125.3 (CH, C-6), 122.3 (C, C-3), 117.6 (CH_2, C-9′), 116.3 (CH_2, C-9), 114.9 (CH, C-3′/C-5′), 110.3 (CH, C-5), 68.9 (CH_2, C-7′), 46.6 (CH_2,C-7), 17.6 (CH_3). HRESIMS *m/z* 280.1732 $[M + H]^+$, calcd for $C_{19}H_{22}NO$ *m/z* 280.1703.

Another fraction of silica gel chromatography, further purified on Sephadex LH-20 (eluted in chloroform), afforded the derivative **10b** (13.0 mg) with 45 % yield. Colourless oil. ^{1}H NMR (500 MHz, $CDCl_3$): δ 7.46 (d, J = 8.7 Hz, 2H, H-2′/H-6′), 7.27 (s, 1H, H-2), 7.25 (d, J = 8.2 Hz, 1H, H-6), 6.96 (d, J = 8.7 Hz, 2H, H-3′/H-5′), 6.74 (d, J = 8.1, 1H, H-5), 6.10 (m, 1H, H-7′), 5.45 (dd, J = 17.2, 1.4 Hz, 1H, H_a-9′), 5.31 (dd, J = 10.5, 1.2 Hz, 1H, H_b-9′), 4.58 (d, J = 5.3 Hz, 2H, H-8′), 2.24 (s, 3H, CH_3). ^{13}C NMR (125 MHz, $CDCl_3$): δ 157.5(C, C-4′), 143.7 (C, C-4), 134.4 (C, C-1′), 133.6 (CH, C-8′), 131.6 (CH, C-1), 129.0 (CH, C-2), 127.5 (CH, C-2′/C-6′), 125.3 (CH, C-6), 122.7 (C, C-3), 117.7 (CH_2, C-9′), 115.4 (CH, C-5), 115.1 (CH, C-3′/C-5′), 69.0 (CH_2, C-7′), 17.7 (CH_3). HRESIMS *m/z* 240.1412 $[M + H]^+$, calcd for $C_{16}H_{18}NO$ *m/z* 240.1388.

4-(Allylamino)-3-methyl-(1,1′-biphenyl)-4′-ol (10c) and 4′-(diallylamino)-3-methyl-(1,1′-biphenyl)-4′-ol (10d). A solution of compound **5** (25.0 mg; 0.12 mmol) in dry acetone (2 mL) was mixed in K_2CO_3 (41.5 mg; 0.30 mmol) for 10 min, then, allyl bromide (36.3; 0.30 mmol) was added, and the mixture was refluxed for 6 h. The mixture was filtered, and silica gel column chromatography (cyclohexane → cyclohexane: acetone 90:10).

10c: 3.0 mg, 11% yield, colourless oil. ^{1}H NMR (500 MHz, $CDCl_3$): δ 7.41 (d, J = 8.3 Hz, 2H, H-2/H-6′), 7.30 (d, J = 7.7 Hz, H-6), 7.26 (s,1H, H-2), 6.85 (d, J = 8.3, 2H, H-3′/H-5′), 6.66 (d, J = 7.9 Hz, H-5), 6.02 (m, 1H, H-8), 5.32 (d, J = 18.2 Hz, 1H, H_a-9), 5.20 (d, J = 10.2 Hz,1H, H_b-9), 3.87 (d, J = 4.9 Hz, 2H, H-7), 2.22 (s, 3H, CH_3). ^{13}C NMR (125 MHz, $CDCl_3$): δ 154.3 (C, C-4′), 145.1 (C, C- 4), 135.6 (CH, C-8), 134.5 (C, C-1′), 129.9 (C, C-1), 128.7 (CH, C-2), 127.7 (CH, C-2′/C-6′), 125.4 (CH, C-6), 122.4 (C, C-3), 116.4 (CH_2, C-9), 115.6 (CH, C-3′/C-5′), 110.5 (CH, C-5), 46.6 (CH_2, C-7), 17.7 (CH_3). HRESIMS *m/z* 240.1411 $[M + H]^+$, calcd for $C_{16}H_{18}NO$ *m/z* 240.1388.

10d: 3.3 mg, 9.2 % yield, yellowish oil. ^{1}H NMR (500 MHz, $CDCl_3$): δ 7.46 (d, J = 8.5 Hz, 2H, H-2′/H-6′), 7.37 (s, 1H, H-2), 7.30 (d, J = 8.3 Hz, 1H, H-6), 7.05 (d, J = 8.3 Hz, 1H, H-5), 6.88 (d, J = 8.5 Hz, H-3′/H-5′), 5.83 (m, 2H, H-8/H-11), 5.20 (d, J = 17.1 Hz, 2H, H_a-9/H_a-12), 5.13 (d, J = 10.2, 2H, H_b-9/H_b-12), 3.62 (d, J = 6.0, 4H, H-7/H-10), 2.38 (s, CH_3). ^{13}C NMR (125 MHz, $CDCl_3$): δ 154.6 (C, C-4′), 148.8 (C, C-4), 135.3 (CH, C-8/C-11), 133.9 (C, C-1/C-1′/C-3), 129.4 (CH, C-2), 128.0 (CH, C-2′/C-6′), 124.1 (CH, C-6), 122.1 (CH, C-5), 117.0 (CH_2, C-9/ C-12), 115.5 (CH, C-3′/C-5′), 55.6 (CH_2, C-7/C-10), 18.5 (CH_3). HRESIMS *m/z* 280.174 $[M + H]^+$, calcd for $C_{19}H_{22}NO$ *m/z* 280.1701.

4′-(Allyloxy)-5-methyl-(1,1′-biphenyl)-2-amine (11). A solution of compound **6** (20.0 mg; 0.10 mmol) in dry acetone (2 mL) was mixed in K_2CO_3 (55.3 mg; 0.40 mmol) for 10 min, then, allyl bromide (60.5 mg; 0.50 mmol) was added, and the mixture was refluxed for 6 h. The mixture was filtered, and the expected compound (8.9 mg, 37 % yield) was recovered after purification on silica gel column chromatography (cyclohexane: acetone 95:5 → cyclohexane: acetone 90:10). Amorphous white solid. ^{1}H NMR (500 MHz, $CDCl_3$): δ 7.37 (d, J = 8.4 Hz, 2H, H-2′/H-6′), 6.99 (d, J = 8.2 Hz, 2H, H-3′/H-5′), 6.93 (s, 1H, H-6), 6.89 (m, 1H, H-4), 6.68 (d; J = 7.9 Hz,1H, H-3), 6.09 (m, 1H, H-8′), 5.45 (d, J = 17.2 Hz, 1H, H_a-9), 5.31 (d, J = 10.3 Hz, 1H, H_b-9), 4.58 (d, J = 5.3 Hz, H-7′), 2.27 (s, 3H, CH_3). ^{13}C NMR (125 MHz, $CDCl_3$): δ 157.9 (C, C-4′), 141.2 (C, C-2), 133.4 (CH, C-8′), 132.2 (C, C-1′), 131.1 (CH, C-6), 130.3 (CH, C-2′/C-6′), 128.8 (CH, C-4), 128.0 (C, C-5), 127.6 (C, C-1), 117.9 (CH_2, C-9′), 115.8 (CH, C-3), 115.1 (CH, C-3′/C-5′), 69.0 (CH_2, C-7′), 20.6 (CH_3). HRESIMS *m/z* 240.1407 $[M + H]^+$ (calcd for $C_{16}H_{18}NO$ *m/z* 240.1389).

2,4′-Bis(allyloxy)-5-nitro-1,1′-biphenyl (13). A solution of compound **7** (16.9 mg; 0.07 mmol) in dry acetone (1 mL) was mixed in K_2CO_3 (40.4 mg; 0.30 mmol) for 10 min, then, allyl bromide (47.2 mg; 0.39 mmol) was added, and the mixture was refluxed for 6 h. The mixture was filtered, and the expected compound (18.8 mg, 82.6 % yield) was recovered after purification on silica gel column chromatography (cyclohexane: acetone 90:10). Yellow solid. ^{1}H NMR (500 MHz, $CDCl_3$): δ 8.22 (dd, J = 2.9,1.0 Hz, 1H, H-6), 8.17 (dd, J = 2.9,0.9 Hz, H-4), 7.50 (d, J = 8.8 Hz, 2H, H-2′/H-6′), 7.00 (d, J = 8.8 Hz, 2H, H-3′/H-5′), 7.00 (d, J = 3.0 Hz, 1H, H-3), 6.09 (m, 1H, H-8′), 5.99 (m, 1H, H-8), 5.45 (d, J = 17.3 Hz, 1H, H_a-9′), 5.37 (d, J = 17.4 Hz, 1H, H_a-9), 5.32 (d, J = 10.5 Hz, 1H, H_b-9′), 5.29 (d, J = 10.5, 1H, H_b-9), 4.67 (d, J = 4.5 Hz, 2H, H-7), 4.59 (d, J = 5.8 Hz, 2H, H-7′). ^{13}C NMR (125 MHz, $CDCl_3$): δ 160.5 (C, C-1), 158.6 (C, C-4′), 141.7 (C, C-5), 133.2 (CH, C-8′), 132.0 (CH, C-8),131.4 (C, C-1′), 130.8 (CH, C-2′/C-6′), 128.7 (C, C-1), 126.3 (CH, C-6), 124.3 (CH, C-4), 118.0 (CH_2, C-9′), 117.9 (CH_2, C-9), 114.6 (CH, C-3′/C-5′), 112.0 (CH, C-3), 69.7 (C, C-7), 69.0(C, C-7′). HRESIMS *m/z* 312.1275 $[M + H]^+$ (calcd for $C_{18}H_{18}NO_4$ *m/z* 312.1236).

***N*-Allyl-2-(allyloxy)-3′-methyl-(1,1′-biphenyl)-4′-amine (13a), 2-(allyloxy)-3′-methyl-(1,1′-biphenyl)-4′-amine (13b) and *N,N*-diallyl-2-(allyloxy)-3′-methyl-(1,1′-biphenyl)-4′-amine (13c)**. A

solution of compound **8** (25.0 mg; 0.12 mmol) in dry acetone (2 mL) was mixed in K_2CO_3 (66.3 mg; 0.48 mmol) for 10 min, then, allyl bromide (72.6 mg; 0.60 mmol) was added and the mixture was refluxed for 7 h. The mixture was filtered, and the expected compound **13a** (10.0 mg, 30 % yield) was recovered after purification on silica gel column chromatography (petroleum ether → petroleum: dichloromethane 35:65). Yellowish oil.^{1}H NMR (500 MHz, $CDCl_3$): δ 7.37 (d, J = 8.3 Hz, 1H, H-6′), 7.34 (d, J = 7.8 Hz, 1H, H-6), 7.33 (s, 1H, H-2′), 7.22 (t, J = 7.8 Hz, 1H, H-4), 7.01(t, J = 7.4 Hz, 1H, H-5), 6.95 (d, J = 8.2 Hz, 1H, H-3), 6.67 (d, J = 8.3 Hz, 1H, H-5′), 6.00 (m, 2H, H-8/H-8′), 5.36 (ddt, J = 17.6, 16.1, 1.6, 2H, H_a-9′/H_a-9), 5.22 (ddt, J = 10.3, 2.6, 1.4 Hz, H_b-9′/H_b-9), 4.55 (d, J = 4.7 Hz, 2H, H-7), 3.88 (d, J = 3.9 Hz, 2H, H-7′), 2.21 (s, 3H, CH_3). ^{13}C NMR (125 MHz, $CDCl_3$): δ 155.4 (C, C-2), 144.9 (C, C-4′), 135.6 (CH, C-8′), 133.6 (CH, C-8), 131.4 (CH, C-2′), 131.3 (C, C-1), 130.6 (CH, C-6), 128.2 (CH, C-6′), 127.4 (CH, C-4), 127.1 (C, C-1′), 121.4 (C, C-3′), 121.1 (CH, C-5), 116.6 (CH_2, C-9), 116.3 (CH_2, C-9′), 113.0 (CH, C-3), 109.6 (C, C-5′), 69.1 (CH_2, C-7), 46.6 (CH_2, C-7′), 17.6 (CH_3). HRESIMS m/z 280.1730 $[M + H]^+$ (calcd for $C_{19}H_{22}NO$ m/z 280.1701).

13b: 5.7 mg, 20 % yield. Colourless oil. ^{1}H NMR (500 MHz, CD_3OD): δ 7.22 (t, J = 7.8 Hz, 1H, H-4), 7.20 (s, 1H, H-2′), 7.16 (t, J = 7.8 Hz, 1H, H-6), 7.15 (d, J = 8.1 Hz, 1H, H-6′), 7.00 (t, J = 7.4 Hz, 1H, H-5), 6.95 (d, J = 7.4 Hz, 1H, H-3), 6.75 (d, J = 8.1 Hz, 1H, H-5′), 5.99 (m, 1H, H-8), 5.35 (d, J = 17.3 Hz, 1H, H_a-9), 5.20 (d, J = 16.6 Hz, 1H, H_b-9), 4.54 (d, J = 4.6 Hz, 2H, H-7), 2.12 (s, 3H, CH_3). ^{13}C NMR (125 MHz, CD_3OD): δ 156.8(C, C-2), 145.4 (C, C-4), 135.0 (CH, C-8), 133.0 (C, C-1′), 132.4 (CH, C-2′), 131.4 (CH, C-6′), 130.2 (C, C-1), 129.0 (CH, C-6), 128.5 (HC, C-4), 123.4 (CH, C-5), 122.2 (C, C-2′), 116.7 (CH_2, C-9), 116.0 (CH, C-5′), 114.5 (CH, C-3), 70.2 (CH_2, C-7), 17.6 (CH_3). HRESIMS m/z 240.1407 $[M + H]^+$ (calcd for $C_{16}H_{18}NO$ m/z 240.1388).

13c: 5.5 mg, 14 % yield. Yellowish oil. ^{1}H NMR (500 MHz, $CDCl_3$): δ 7.39 (d, J = 1.7 Hz, 1H, H-2′), 7.33 (d, J = 1.7 Hz, 1H, H-6′), 7.32 (d, J = 7.6 Hz, 1H, H-6), 7.23 (d, J = 1.3 Hz, 1H, H-5′), 7.02 (t, J = 7.5, Hz, 1H, H-4/H-5), 6.95 (d, J = 8.1 Hz, 1H, H-3), 5.93 (m, 1H, H-8), 5.76 (m, 2H, H-8′/ H-11′), 5.27(dd, J = 17.3, 1.7 Hz, 1H, H_a-9), 5.12 (dd, J = 9.1, 1.5 Hz, 2H, H_a-9′/H $_a$ −12′), 5.05 (dd, J = 10.2, 1.3 Hz,2H, H_b-9/H_b-9′), 4.46 (d, J = 4.7 Hz, 2H, H-7), 3.55 (d, J = 6.1 Hz, 4H, H-7′/ H-10′), 2.28 (s,3H, CH_3). ^{13}C NMR (125 MHz, $CDCl_3$): δ 155.5 (C, C-2), 148.9 (C, C-2′), 135.5(CH, C-8′/ C-11′), 133.4 (CH, C-8), 132.9 (C, C-1), 132.8 (CH, C-2′), 132.3(C, C-1′), 131.0 (C, C-3′), 130.8 (CH, C-5), 127.9 (CH, C-5′), 127.1 (CH, C-6′), 121.2 (CH, C-4), 121.1 (HC, C5), 116.9 (CH_2, C-9′/ C-12′), 116.6 (CH_2, C-9), 113.0 (CH, C-3), 69.0 (CH_2, C-7), 55.3 (CH_2, C-7′/ C-10′), 18.4 (CH_3). HRESIMS m/z 320.2044 $[M + H]^+$ (calcd for $C_{22}H_{26}NO$ m/z 320.2014).

***N,N*-Diallyl-2-(allyloxy)-3′-methyl-(1,1′-biphenyl)-6′-amine (14)**. A solution of compound **9** (50.0 mg; 0.25 mmol) in dry acetone (3.5 mL) was mixed in K_2CO_3 (103.7 mg; 0.75 mmol) for 10 min, then allyl bromide (90.7 mg; 0.75 mmol) and the mixture was refluxed for 24 h. The mixture was filtered, and the expected compound (12.0 mg, 15 % yield) was recovered after reversed-phase C18 column chromatography (water-acetonitrile 60:40 → acetonitrile. Brownish oil.^{1}H NMR. (500 MHz, $CDCl_3$): δ 7.24 (d, J = 7.5 Hz, 1H, H-6), 7.24 (t, J = 7.4 Hz, 1H, H-4), 7.03 (s, 1H, H-2′), 7.04 (d, J = 8.2 Hz, 1H, H-5′), 6.97 (t, J = 7.4 Hz, 1H, H-5), 6.93 (dd, J = 8.1, 2.3 Hz, 1H, H-3/H-4′), 6.92 (d, J = 2.5 Hz, 1H, H-3), 5.91(m, 1H, H-8), 5.52 (m, 2H, H-8′/ H-11′), 5.21 (dd, J = 17.3, 1.5 Hz, 1H, H_a-9), 5.13 (dd, J = 17.3, 1.2 Hz, 2H, H $_a$-9′ / H $_a$-12′), 5.00 (dd, J = 10.1, 1.5 Hz, 1H, H_b-9), 4.96 (dd, J = 10.3, 1.2 Hz, 2H, H_b-9′/ H_b-12′), 4.50 (d, J = 4.7 Hz, 2H, H-7′), 3.39 (d, J = 6.2, 2H, H-7′/H-10′), 2.29 (s, 3H, CH_3). ^{13}C NMR (125 MHz, $CDCl_3$): δ 155.7 (C, C-2), 147.3 (C, C-6′), 135.9 (CH, C-8′/ C-11′), 133.7 (CH, C-8), 133.7 (C, C-1′), 132.8 (CH, C-5′), 131.9 (C,C-6), 131.1 (C, C-3′), 130.9 (C, C-1), 128.1 (CH, C-2′), 128.0 (CH, C-4), 121.1 (CH, C-4′), 120.5 (CH, C-5), 116.6 (CH_2, C-9′/C-12′), 116.6 (CH_2, C-9), 112.5 (CH, C-3), 68.7 (CH_2, C-7), 55.4 (CH_2, C-7′/C-10′), 21.0 (CH_3). HRESIMS m/z 320.2055 $[M + H]^+$ (calcd for $C_{22}H_{26}NO$ m/z 320.2014).

4.2.4. General procedure for Claisen rearrangement

A 1 M Et_2AlCl solution (in *n*-hexane; 100 μL) was added dropwise to allyl derivatives **10**–**13** in dry CH_2Cl_2 (1 mL). The mixture was stirred at room temperature for 2–3 h, and then the reaction was quenched by adding 2 N HCl solution (2 mL) at 0 °C temperature. The mixture was partitioned with CH_2Cl_2 (2 × 5 mL); the combined organic phases were washed with water, dried over anhydrous Na_2SO_4, filtered and taken to dryness. The expected compound was recovered after column chromatography, affording the pure products.

3′-Allyl-4-(allylamino)-3-methyl-(1,1′-biphenyl)-4′-ol (15a). Compound **15a** (5.0 mg, 51 % yield) was recovered after a Sephadex LH-20 column chromatography (dichloromethane). Yellowish oil. ^{1}H NMR (500 MHz, $CDCl_3$): δ 7.32 (d, J = 8.2 Hz, 1H, H-2′/H-6), 7.28 (s, 1H, H-6′/H-2), 6.85 (d, J = 8.1 Hz, 1H, H-3′), 6.67 (d, J = 8.1 Hz, 1H, H-5), 6.05 (m, 2H, H-8/H-8′), 5.33 (dd, J = 17.2,1.4 Hz, 1H, H_a-9), 5.21 (m, 3H, H_b-9$_b$ / H $_a$-9′/ H_b-9′), 3.88 (d, J = 5.3 Hz, 2H, H-7), 3.48 (d, J = 6.3 Hz, 2H, H-7′), 2.23 (s, 3H, CH_3). ^{13}C NMR (125 MHz, $CDCl_3$): δ 153.2 (C, C-4′), 145.4 (C-4), 136.9 (CH, C-8′), 135.9 (CH, C-8), 134.9 (C, C-1′), 130.3 (C, C-1), 129.0 (CH, C-2), 128.9 (CH, C-6′), 126.2 (CH, C-6), 125.7 (CH, C-2′), 125.7 (C, C-5), 122.7 (C, C-3), 116.9 (CH_2, C-9′), 116.7 (CH_2, C-9), 116.5 (CH, C-3′), 110.8 (CH, C-5), 47.0 (CH_2, C-7), 35.8 (CH_2, C-7′), 18.0 (CH_3). HRESIMS m/z 280.1680 $[M + H]^+$, calcd for $C_{19}H_{22}NO$ m/z 280.1702.

3′-Allyl-4-amino-3-methyl-(1,1′-biphenyl)-4′-ol (15b). Compound **15b** was achieved without further purification (3.6 mg, 60 % yield). Colourless oil. ^{1}H NMR (500 MHz, $CDCl_3$): δ 7.29 (d, J = 8.3 Hz, 1H, H-6′), 7.28 (s,1H, H-2′), 7.25 (s, 1H, H-2), 7.23 (d, J = 8.3 Hz, 1H, H-6), 6.84 (d, J = 8.1 Hz, 1H, H-5′), 6.72 (d, J = 8.0 Hz, 1H, H-5), 6.05 (m, 1H, H-7′), 5.20 (d, J = 17.3 Hz, 1H, H_a-9′), 5.17 (d, J = 10.1 Hz, 1H, H_b-9′), 3.46 (d, J = 6.1 Hz, 2H), 2.22 (s,3H, CH_3). ^{13}C NMR (125 MHz, $CDCl_3$): δ 153.0 (C, C-4′), 143.7 (C, C-4), 136.6 (CH_2, C-8′), 134.5 (C, C-1′), 131.7 (C, C-1), 131.6 (C, C-3′), 129.0 (CH, C-2), 128.7 (CH, C-2′), 125.9 (CH, C-6′), 125.5 (C, C-3), 125.4 (CH, C-6), 116.7 (CH_2, C-9′), 116.2 (CH, C-5′), 115.4 (CH, C-5), 35.4 (C CH_2, C-7′), 17.7 (CH_3). HRESIMS m/z 240.1352 $[M + H]^+$ (calcd for $C_{16}H_{18}NO$ m/z 240.1388).

3′-Allyl-2-amino-5-methyl-(1,1′-biphenyl)-4′-ol (16). The expected compound **16** (8.0 mg, 50 % yield) was recovered after silica gel column chromatography (cyclohexane → cyclohexane: acetone 100 → 50:50). Amorphous white solid. ^{1}H NMR (500 MHz, $CDCl_3$): δ 7.21 (s, 1H, H-2′), 7.20 (d, J = 7.8 Hz, 1H, H-6′), 6.94 (d, J = 8.3 Hz, 1H, H-4), 6.92 (s, 1H, H-6), 6.86 (d, J = 7.8 Hz, 1H, H-5′), 6.68 (d, J = 7.9 Hz, 1H, h-3), 6.04 (ddt, J = 16.6, 10.1, 6.4 Hz, 1H, H-8′), 5.19 (d, J = 17.4 Hz, 1H, H_a-9′), 5.16 (d, J = 10.1 Hz, 1H, H_b-9′), 3.44 (d, J = 6.2 Hz, 2H, H-7′), 2.26 (s, 3H, CH_3). ^{13}C NMR (125 MHz, $CDCl_3$): δ 153.4 (C, C-4′), 141.1 (C, C-2),136.4 (C, C-8′), 132.3 (C, C-5), 131.2 (C, C-6), 131.1 (C, C-2′), 128.8 (C, C-4), 128.6 (C, C-6′), 128.1 (C, C-1′), 125.8 (C, C-3′), 116.7 (C, C-9′), 116.2 (C, C-5′), 115.9 (C, C-3), 35.3 (C, C-7′), 20.6 (C, CH_3). HRESIMS m/z 240.1403 $[M + H]^+$ (calcd for $C_{16}H_{18}NO$ m/z 240.1388).

3-Allyl-4′-(allylamino)-3′-methyl-(1,1′-biphenyl)-2-ol (17a). Compound **17a** (5.6 mg, 25 % yield) was recovered after silica gel column chromatography (petroleum ether: dichloromethane 95:5 → 90:10). Yellowish oil. ^{1}H NMR (500 MHz, $CDCl_3$): δ 7.20 (dd, J = 8.2,1.8 Hz, 1H, H-6′), 7.15(s, 1H, H-2′), 7.08 (d, J = 7.6 Hz, 2H, H-4/H-6), 6.89 (t, J = 7.5 Hz, 1H, H-5), 6.70 (d, J = 8.2 Hz, 1H, H-5′), 6.05 (m, 2H, H-8/H-8′), 5.33(dd, J = 17.3, 1.3 Hz, 1H, H_a-9′), 5.22 (dd, J = 10.3, 1.1 Hz, 1H, H_b-9′), 5.13 (dd, J = 17.1, 1.6 Hz, 1H, H_a-9), 5.09 (dd, J = 10.0, 1.1 Hz, 1H, H_b-9), 3.88(d, J = 5.2 Hz, 2H, H-7′), 3.46 (d, J = 6.5 Hz, 2H, H-7), 2.21 (s, 3H, CH_3). ^{13}C NMR (125 MHz, $CDCl_3$): δ 150.7 (C, C-2), 145.8 (C, C-4′), 137.1 (CH, C-8), 135.4 (CH, C-8′), 131.0 (CH, C-2′), 128.9 (CH, C-4), 128.5 (C,C-1), 128.3 (CH, C-6), 127.9 (CH,C-6′), 126.3 (C, C-3), 125.4 (C, C-1′), 123.0 (C, C-3′), 120.3 (CH, C-5), 116.6 (CH_2, C-9′), 115.7 (CH_2, C-9), 110.7 (CH, C-5′), 46.6 (CH_2, C-7′), 34.9 (CH_2, C-7), 17.6 (CH_3). HRESIMS m/z 280.1685 $[M + H]^+$ (calcd for $C_{19}H_{22}NO$ m/z 280.1701).

3-Allyl-4′-amino-3′-methyl-(1,1′-biphenyl)-2-ol (17b). The

expected compound **17b** (3.1 mg) was achieved with 72 % yield after liquid–liquid partition. ^{1}H NMR (500 MHz, $CDCl_3$): δ 7.17 (s, 1H, H-2′), 7.13 (d, J = 8.1 Hz, 1H, H-6′), 7.08 (t, J = 8.5 Hz, 1H, H-5), 7.09 (d, J = 8.9 Hz, 1H, H-6), 6.90 (d, J = 7.9 Hz, 1H, H-4), 6.87 (d, J = 7.9 Hz, 1H, H-5′), 6.03 (m, 1H, H-8), 5.13 (d, J = 17.1 Hz, 1H, H_a-9), 5.09 (d, J = 10.0 Hz, 1H, H_b-9), 3.45 (d, J = 6.3 Hz, 2H, H-7), 2.26 (s, 3H, CH_3). ^{13}C NMR (125 MHz, $CDCl_3$): δ 150.5 (C, C-2), 142.8 (C, C-4′), 136.8 (CH_2, C-9), 131.3 (CH, C-2′), 129.1 (CH, C-5), 128.2 (CH, C-6), 128.2 (C, C-1), 127.8 (CH, C-6′), 126.2 (C, C-3), 124.1 (C, C-1′/C-3′), 120.2 (CH, C-4), 116.4 (CH, C-5′), 115.7 (CH_2, C-8), 34.8 (CH_2, C-7), 17.5 (CH_3). HRESIMS m/z 240.1357 $[M + H]^+$ (calcd for $C_{16}H_{18}NO$ m/z 240.1388).

3-Allyl-4′-(diallylamino)-3′-methyl-(1,1′-biphenyl)-2-ol (17c). The expected compound **17c** (6.7 mg, 50 % yield) was recovered after silica gel column chromatography (petroleum ether 100%). Brownish oil. ^{1}H NMR (500 MHz, $CDCl_3$): δ 7.26 (s, 1H, H-2′), 7.20 (d, J = 6.4 Hz, 1H, H-6′), 7.10 (m, 3H, H-4/H-6/H-5′), 6.91 (t, J = 7.5 Hz, 1H, H-5), 6.06 (ddt, J = 16.7, 10.6, 6.6 Hz, 1H, H-8), 5.82 (ddt, J = 16.4, 10.4, 6.1 Hz, 2H, H-8′/H-11′), 5.21 (dd, J = 17.2, 1.2 Hz, 2H, H_a-9′ /H_a-12′), 5.14 (d, J = 11.7 Hz, 2H, H_b-9′/H_b-12′), 5.13 (d, J = 16.2 Hz, 1H, H_a-9), 5.10 (d, J = 10.1 Hz, 1H, H_b-9), 3.63 (d, J = 6.0 Hz, 4H, H-7′), 3.46 (d, J = 6.8 Hz, 2H, H-7), 2.36 (s, 3H, CH_3). ^{13}C NMR (125 MHz, $CDCl_3$): δ 150.6 (C, C-2), 149.9 (C, C-4′), 137.0 (CH, C-8), 135.3 (CH, C-8′/ C-11′), 134.6 (C, C-3′), 132.0 (CH, C-2′), 131.5 (C, C-1′), 129.4 (CH, C-4), 128.4 (CH, C-6), 128.2 (C, C-1), 126.8 (CH, C-6′), 126.4 (C, C-3), 122.6 (CH, C-5′), 120.4 (CH, C-5), 117.4 (CH_2, C-9′/C-12′), 115.8 (CH_2, C-9), 55.6 (CH_2, C-7′/C-10′), 34.9 (CH_2, C-7), 18.7 (CH_3). HRESIMS m/z 320.1985 $[M + H]^+$ (calcd for $C_{16}H_{18}NO$ m/z 320.2014).

4.3. Measurements of pancreatic lipase (PL) inhibition

The inhibition of pancreatic lipase from *porcine pancreas* [EC 3.1.1.3; triacylglycerol acyl hydrolase] was performed employing 4-nitrophenyl butyrate as a substrate.[36] In a 96-well microplate, 150 μL of phosphate buffer (50 mM, pH = 7.2), the PL solution (5 mg/mL in phosphate buffer; 15 μL), and different aliquots (4, 6, 8, 10, and 15 μL) of tested compounds **5 – 17c** (stock solutions were prepared in MeOH ranging from 1.79 mM to 0.96 mM) or of orlistat (6.7 μM in buffer) were mixed. The reactions were incubated at 37 °C for 10 min. Then, the substrate *p*-nitrophenyl butyrate (3.2 mM in H_2O: DMF 70:30, 10 μL) was added, and the microplate was incubated at 37 °C for 30 min under moderate shaking. The plate measurements were acquired at 405 nm. Orlistat was used as a positive reference.

The following equation gave the inhibition percentage of enzyme activity and was employed to elaborate the data for both PL.

$$\%inhibition = \frac{OD_{\text{control}} - OD_{\text{sample}}}{OD_{\text{control}}} * 100$$

where $OD_{control}$ represents the measured optical density for the enzyme-substrate mixture in the absence of an inhibitor, and OD_{sample} represents the optical density of the reaction mixture in the presence of the inhibitor. The concentration required to inhibit the 50% activity of the enzyme (IC_{50}) was calculated by linear regression analysis. The in vitro assay results are reported in Table 2 as IC_{50} values.

4.4. Kinetics of pancreatic lipase inhibition

The mode of inhibition of PL in the presence of tested neolignans was determined spectroscopically [31]. The experiments were performed in 96-well plates employing the enzyme (120 U/mL in phosphate buffer; 10 μL), the selected molecules, and the increasing concentrations of *p*-nitrophenyl butyrate (from 0.3 to 1.9 mM) in a final volume of 200 μL. The optimal concentration of tested compounds was chosen based on the IC_{50} values. The absorbance was read at 405 nm every 1 min for 45 min at 37 °C.

The inhibition constants were calculated from the equations.

$$v_0 = \frac{v_{\max} S}{K_m\left(1 + \frac{I}{Ki}\right) + S}$$

$$v_0 = \frac{v_{\max} S}{K_m\left(1 + \frac{I}{Ki}\right) + S\left(1 + \frac{I}{K'i}\right)}$$

where v_0 is the initial velocity in the absence and presence of the inhibitor, S and I are the substrate and inhibitor concentrations, respectively; v_{max} is the maximum velocity, K_m is the Michaelis-Menten constant, K_i is the competitive inhibition constant, and K'_i is the uncompetitive inhibition constant. The graphs of slope and *y*-intercept of Lineweaver-Burk plots versus the inhibitor concentration gave a straight line, whose intercept corresponds to K_i and K'_i values, respectively.

4.5. Molecular docking analysis

The.sdf files of orlistat, magnolol, and honokiol were downloaded from PubChem (https://pubchem.ncbi.nlm.nih.gov/, I.D. cod respectively: 3034010, 72300, 72303). Meanwhile, the other ligands, namely, the biphenyls **5**–**17**, were drawn by Chemdraw and saved in.sdf files. The 3D models were geometrically minimised with optimised potential liquid simulation (OPLS3) force fields considering the protonation state at pH of 7.0 ± 1 and processed using LigPrep interfaced with Maestro (Version 11) of Schröedinger suite [40].

The minimised geometries were converted into.pdbqt files by Autodock Tools (1.5.6). The 3D structure of pancreatic lipase (PDB ID: 1LPB) was downloaded from Protein Data Bank (RCSB Protein Data Bank: https://www.rcsb.org/structure/ 1lpb accessed April 2020). The lipase is cocrystallised with colipase in the presence of methoxy undecyl phosphonic acid (MUP) as an inhibitor and β-octylglucoside (BOG) as a surfactant. Protein was prepared with Protein wizard, MUP, and BOG, and H_2O molecules were removed; then, the.pdb file obtained was processed with Autodock Tools 1.5.6 and converted in.pdbqt file, merging nonpolar hydrogens and adding Gasteiger charges. The molecular docking studies were performed using Glide Ligand Docking interfaced with Maestro and Autodock Vina software 1.5.6. [41,42] Autogrid4 (4.2.6 version) was used to generate the gridmaps used in the Vina calculations. The grid box was centred in the protein's binding site, with grid coordinates of 50 × 40 × 50 $Å^3$ for x, y, and z, respectively. The spacing between the grid coordinates was 0.708 Å. The grid centre was set to 7.500, 26.042, and 47.696 Å. Receptor grid generation interfaced with Maestro was used to generate the gridmaps for the Glide calculations. The grid box was centred in the protein's binding site, with the grid centre set to 6.52, 22.27 and 43.85 Å. For the docking experiments carried out with AD4, the Lamarckian Genetic Algorithm was chosen to search for the best conformers. During the docking process, a maximum of 10 conformers was considered for each ligand. In Docking calculation, ligands were treated as flexible while protein was treated as rigid. Autodock Vina and Glide were compiled and run in O.S.X. Yosemite (10.10.5) environment. The analysis of docking outcomes was carried out by Maestro (Version 11), and figures of 3D models were generated by Pymol (2.3.5).

Declaration of Competing Interest

The authors declare that they have no known competing financial interests or personal relationships that could have appeared to influence the work reported in this paper.

Data availability

Data will be made available on request.

Acknowledgements

The authors gratefully acknowledge the Bio-Nanotech Research and Innovation Tower of the University of Catania (BRIT; project PONa3_00136) financed by the Italian Ministry for Education, University and Research MIUR, for making available the Synergy H1 microplate reader.

Funding

This research was funded by MIUR ITALY PRIN 2017 (Project No. 2017A95NCJ)

Appendix A. Supplementary data

Supplementary data to this article can be found online at https://doi.org/10.1016/j.bioorg.2023.106455.

References

[1] Y.J. Lee, Y.M. Lee, C.K. Lee, J.K. Jung, S.B. Han, J.T. Hong, Therapeutic applications of compounds in the Magnolia family, Pharmacol. Ther. 130 (2) (2011) 157–176.
[2] L.G. Bjerregaard, B.W. Jensen, L. Angquist, M. Osler, T.I.A. Sorensen, J.L. Baker, Change in Overweight from Childhood to Early Adulthood and Risk of Type 2 Diabetes, N. Engl. J. Med. 378 (14) (2018) 1302–1312.
[3] P. Latino-Martel, V. Cottet, N. Druesne-Pecollo, F.H.F. Pierre, M. Touillaud, M. Touvier, M.P. Vasson, M. Deschasaux, J. Le Merdy, E. Barrandon, R. Ancellin, Alcoholic beverages, obesity, physical activity and other nutritional factors, and cancer risk: A review of the evidence, Critical Reviews in Oncology, Hematology 99 (2016) 308–323.
[4] T. Burki, European Commission classifies obesity as a chronic disease, Lancet Diabetes Endocrinol. 9 (7) (2021) 418.
[5] T.T. Liu, X.T. Liu, Q.X. Chen, Y. Shi, Lipase Inhibitors for Obesity: A Review, Biomed. Pharmacother. 128 (2020).
[6] S.N.C. Sridhar, S. Palawat, A.T. Paul, Design, synthesis, biological evaluation and molecular modelling studies of indole glyoxylamides as a new class of potential pancreatic lipase inhibitors, Bioorg. Chem. 85 (2019) 373–381.
[7] C.Y. Hsu, G.M. Lin, S.T. Chang, Hypoglycemic activity of extracts of Chamaecyparis obtusa var. formosana leaf in rats with hyperglycemia induced by high-fat diets and streptozotocin, J. Tradit. Complement. Med. 10 (4) (2020) 389–395.
[8] B.M. Cheung, T.T. Cheung, N.R. Samaranayake, Safety of antiobesity drugs, Therap. Adv. Drug Safety 4 (4) (2013) 171–181.
[9] A. Korkmaz, E. Bursal, An in vitro and in silico study on the synthesis and characterization of novel bis(sulfonate) derivatives as tyrosinase and pancreatic lipase inhibitors, J. Mol. Struct. 1259 (2022).
[10] A. Korkmaz, E. Bursal, Benzothiazole sulfonate derivatives bearing azomethine: Synthesis, characterization, enzyme inhibition, and molecular docking study, J. Mol. Struct. 1257 (2022).
[11] N. Turan, K. Buldurun, E. Bursal, G. Mahmoudi, Pd(II)-Schiff base complexes: Synthesis, characterization, Suzuki-Miyaura and Mizoroki-Heck cross-coupling reactions, enzyme inhibition and antioxidant activities, J. Organomet. Chem. 970 (2022).
[12] H.Q. Fei, M.X. Li, W.J. Liu, L. Sun, N. Li, L. Cao, Z.Q. Meng, W.Z. Huang, G. Ding, Z. Z. Wang, W. Xiao, Potential lipase inhibitors from Chinese medicinal herbs, Pharm. Biol. 54 (12) (2016) 2845–2850.
[13] Q. Xu, L.T. Yi, Y. Pan, X. Wang, Y.C. Li, J.M. Li, C.P. Wang, L.D. Kong, Antidepressant-like effects of the mixture of honokiol and magnolol from the barks of Magnolia officinalis in stressed rodents, Prog. Neuropsychopharmacol. Biol. Psychiatry 32 (3) (2008) 715–725.
[14] M.H. Pan, Inhibitory effect of magnolol on TPA-induced skin inflammation and tumor promotion in mice, Abstr. Pap. Am. Chem. Soc. 241 (2011).
[15] H.C. Ou, F.P. Chou, T.M. Lin, C.H. Yang, W.H.H. Sheu, Protective effects of honokiol against oxidized LDL-induced cytotoxicity and adhesion molecule expression in endothelial cells, Chem. Biol. Interact. 161 (1) (2006) 1–13.
[16] Z.L. Kong, S.C. Tzeng, Y.C. Liu, Cytotoxic neolignans: an SAR study, Bioorg. Med. Chem. Lett. 15 (1) (2005) 163–166.
[17] D. Lin, Z.Z. Yan, A.Y. Chen, J. Ye, A.X. Hu, J. Liu, J.M. Peng, X.Y. Wu, Anti-proliferative activity and structure-activity relationship of honokiol derivatives, Bioorg. Med. Chem. 27 (16) (2019) 3729–3734.
[18] S. Di Micco, L. Pulvirenti, I. Bruno, S. Terracciano, A. Russo, M.C. Vaccaro, D. Ruggiero, V. Muccilli, N. Cardullo, C. Tringali, R. Riccio, G. Bifulco, Identification by Inverse Virtual Screening of magnolol-based scaffold as new tankyrase-2 inhibitors, Bioorg. Med. Chem. 26 (14) (2018) 3953–3957.
[19] N. Cardullo, V. Barresi, V. Muccilli, G. Spampinato, M. D'Amico, D.F. Condorelli, C. Tringali, Synthesis of Bisphenol Neolignans Inspired by Honokiol as Antiproliferative Agents, Molecules 25 (3) (2020) 17.
[20] L. Pulvirenti, V. Muccilli, N. Cardullo, C. Spatafora, C. Tringali, Chemoenzymatic Synthesis and alpha-Glucosidase Inhibitory Activity of Dimeric Neolignans Inspired by Magnolol, J. Nat. Prod. 80 (5) (2017) 1648–1657.
[21] S. Jada, M.R. Doma, P.P. Singh, S. Kumar, F. Malik, A. Sharma, I.A. Khan, G. N. Qazi, H.M.S. Kumar, Design and synthesis of novel magnolol derivatives as potential antimicrobial and antiproliferative compounds, Eur. J. Med. Chem. 51 (2012) 35–41.
[22] L. Ma, J.Y. Chen, X.W. Wang, X.L. Liang, Y.F. Luo, W. Zhu, T.N. Wang, M. Peng, S. C. Li, S. Jie, A.H. Peng, Y.Q. Wei, L.J. Chen, Structural Modification of Honokiol, a Biphenyl Occurring in Magnolia officinalis: the Evaluation of Honokiol Analogues as Inhibitors of Angiogenesis and for Their Cytotoxicity and Structure-Activity Relationship, J. Med. Chem. 54 (19) (2011) 6469–6481.
[23] B. Taferner, W. Schuehly, A. Huefner, I. Baburin, K. Wiesner, G.F. Ecker, S. Hering, Modulation of GABA(A)-Receptors by Honokiol and Derivatives: Subtype Selectivity and Structure-Activity Relationship, J. Med. Chem. 54 (15) (2011) 5349–5361.
[24] F.M. Djeujo, E. Ragazzi, M. Urettini, B. Sauro, E. Cichero, M. Tonelli, G. Froldi, Magnolol and Luteolin Inhibition of alpha-Glucosidase Activity: Kinetics and Type of Interaction Detected by In Vitro and In Silico Studies, Pharmaceuticals 15 (2) (2022).
[25] V.N. Hamdan II, Y.M. Kasabri, D. Al-Hiari, H. El-Sabawi, Zalloum, Pancreatic lipase inhibitory activity of selected pharmaceutical agents, Acta Pharm. 69 (1) (2019) 1–16.
[26] B.J. Reizman, Y.M. Wang, S.L. Buchwald, K.F. Jensen, Suzuki-Miyaura cross-coupling optimization enabled by automated feedback, React. Chem. Eng. 1 (6) (2016) 658–666.
[27] R.A. Altman, S.L. Buchwald, Pd-catalyzed Suzuki-Miyaura reactions of aryl halides using bulky biarylmonophosphine ligands, Nat. Protoc. 2 (12) (2007) 3115–3121.
[28] T.E. Barder, S.D. Walker, J.R. Martinelli, S.L. Buchwald, Catalysts for Suzuki-Miyaura coupling processes: Scope and studies of the effect of ligand structure, J. Am. Chem. Soc. 127 (13) (2005) 4685–4696.
[29] J.Y. Cho, G.B. Roh, E.J. Cho, Visible-Light-Promoted Synthesis of Dibenzofuran Derivatives, J Org Chem 83 (2) (2018) 805–811.
[30] M. Sanchez-Peris, J. Murga, E. Falomir, M. Carda, J.A. Marco, Synthesis of honokiol analogues and evaluation of their modulating action on VEGF protein secretion and telomerase-related gene expressions, Chem. Biol. Drug Des. 89 (4) (2017) 577–584.
[31] L.G. Beholz, J.R. Stille, Lewis acid-promoted 3-aza-cope rearrangement of n-alkyl-n-allylanilines, J. Org. Chem. 58 (19) (1993) 5095–5100.
[32] P. Mondal, L. Thander, S.K. Chattopadhyay, A new entry to the phenanthridine ring system, Tetrahedron Lett. 53 (11) (2012) 1328–1331.
[33] A. Chaskar, V. Padalkar, K. Phatangare, K. Patil, A. Bodkhe, B. Langi, Heteropoly acids as useful recyclable heterogeneous catalysts for the facile and highly efficient aza-cope rearrangement of N-allylanilines, Appl. Catal. A-General 359 (1–2) (2009) 84–87.
[34] S. Tripathi, M.H. Chan, C.P. Chen, An expedient synthesis of honokiol and its analogues as potential neuropreventive agents, Bioorg. Med. Chem. Lett. 22 (1) (2012) 216–221.
[35] N. Cardullo, G. Floresta, A. Rescifina, V. Muccilli, C. Tringali, Synthesis and in vitro evaluation of chlorogenic acid amides as potential hypoglycemic agents and their synergistic effect with acarbose, Bioorg. Chem. 117 (2021).
[36] N. Cardullo, V. Muccilli, L. Pulvirenti, C. Tringali, Natural Isoflavones and Semisynthetic Derivatives as Pancreatic Lipase Inhibitors, J. Nat. Prod. 84 (3) (2021) 654–665.
[37] A. Daina, O. Michielin, V. Zoete, SwissADME: a free web tool to evaluate pharmacokinetics, drug-likeness and medicinal chemistry friendliness of small molecules, Sci. Rep. 7 (2017).
[38] A. Daina, O. Michielin, V. Zoete, iLOGP: A Simple, Robust, and Efficient Description of n-Octanol/Water Partition Coefficient for Drug Design Using the GB/SA Approach, J. Chem. Inf. Model. 54 (12) (2014) 3284–3301.
[39] Y.C. Martin, A bioavailability score, J. Med. Chem. 48 (9) (2005) 3164–3170.
[40] E. Harder, W. Damm, J. Maple, C.J. Wu, M. Reboul, J.Y. Xiang, L.L. Wang, D. Lupyan, M.K. Dahlgren, J.L. Knight, J.W. Kaus, D.S. Cerutti, G. Krilov, W. L. Jorgensen, R. Abel, R.A. Friesner, OPLS3: A Force Field Providing Broad Coverage of Drug-like Small Molecules and Proteins, J. Chem. Theory Comput. 12 (1) (2016) 281–296.
[41] W.Z. Tang, J.T. Liu, Q. Hu, R.J. He, X.Q. Guan, G.B. Ge, H. Han, F. Yang, H.W. Lin, Pancreatic Lipase Inhibitory Cyclohexapeptides from the Marine Sponge-Derived Fungus Aspergillus sp. 151304, J. Nat. Prod. 83 (7) (2020) 2287–2293.
[42] H.M.T. Vu, D.D. Vu, V.D. Truong, T.V.P. Nguyen, T.D. Tran, Virtual Screening, oriented-synthesis and evaluation of lipase inhibitory Activity of benzyl Amino chalcone derivatives, J. Med. Pharm. Res. 1 (2017) 26–36.